ปฏิกิริยาคาร์บอนไดออกไซด์รีฟอร์มมิงของมีเทนบนตัวเร่งปฏิกิริยานิกเกิล โคบอลต์บนตัวรองรับอะลูมินา-ซีโอไลต์ชนิด HY

นางสาวทิพย์เนตร เชาวน์วานิชย์

วิทยานิพนธ์นี้เป็นส่วนหนึ่งของการศึกษาตามหลักสูตรปริญญาวิศวกรรมศาสตรมหาบัณฑิต
สาขาวิชาวิศวกรรมเคมี ภาควิชาวิศวกรรมเคมี
คณะวิศวกรรมศาสตร์ จุฬาลงกรณ์มหาวิทยาลัย
ปีการศึกษา 2558

Carbon dioxide reforming of methane over Ni-Co catalysts supported on Al_2O_3-HY zeolite

Miss Tipanate Chaovanich

A Thesis Submitted in Partial Fulfillment of the Requirements
for the Degree of Master of Engineering Program in Chemical Engineering
Department of Chemical Engineering
Faculty of Engineering
Chulalongkorn University
Academic Year 2015

Thesis Title	Carbon dioxide reforming of methane over Ni-Co catalysts supported on Al_2O_3-HY zeolite
By	Miss Tipanate Chaovanich
Field of Study	Chemical Engineering
Thesis Advisor	Assistant Professor Suphot Phatanasri, D.Eng.

Accepted by the Faculty of Engineering, Chulalongkorn University in Partial Fulfillment of the Requirements for the Master's Degree

.....Dean of the Faculty of Engineering

(Associate Professor Supot Teachavorasinskun, D.Eng.)

THESIS COMMITTEE

.....Chairman

(Associate Professor Joongjai Panpranot, Ph.D.)

.....Thesis Advisor

(Assistant Professor Suphot Phatanasri, D.Eng.)

.....Examiner

(Chutimon Satirapipathkul, D.Eng.)

.....External Examiner

(Assistant Professor Soipatta Soisuwan, D.Eng.)

ทิพย์เนตร เชาวน์วานิชย์ : ปฏิกิริยาคาร์บอนไดออกไซด์รีฟอร์มมิงของมีเทนบนตัวเร่งปฏิกิริยานิกเกิล โคบอลต์บนตัวรองรับอะลูมินา-ซีโอไลต์ชนิด HY (Carbon dioxide reforming of methane over Ni-Co catalysts supported on Al_2O_3-HY zeolite) อ. ที่ปรึกษาวิทยานิพนธ์หลัก: ผศ. ดร.สุพจน์ พัฒนะศรี, 93 หน้า.

ในงานวิจัยนี้ได้ทำการศึกษาผลของอัตราส่วนซิลิกาต่ออะลูมินา (15, 200 และ 500) ของซีโอไลต์ชนิด HY ในตัวเร่งปฏิกิริยาโลหะผสมนิกเกิล โคบอลต์บนตัวรองรับอะลูมินา-ซีโอไลต์ชนิด HY ที่ถูกเตรียมโดยวิธีการเคลือบฝังแบบเปียก นอกจากนี้ยังศึกษาผลของอัตราส่วนของตัวรองรับอะลูมินาและซีโอไลต์ชนิด HY ในตัวเร่งปฏิกิริยาโลหะผสมนิกเกิล โคบอลต์ด้วยอัตราส่วนของตัวรองรับดังนี้ 3:1, 1:1 และ 1:3 และเปรียบเทียบกับตัวรองรับอะลูมินาและซีโอไลต์ชนิด HY ในตัวเร่งปฏิกิริยาโลหะผสมนิกเกิล-โคบอลต์ ตัวเร่งปฏิกิริยาทั้งหมดถูกทดสอบในปฏิกิริยาคาร์บอนไดออกไซด์รีฟอร์มมิงของมีเทนที่อุณหภูมิ 700 องศาเซลเซียสภายใต้ความดันบรรยากาศและวิเคราะห์คุณลักษณะด้วยเทคนิคต่างๆ จากผลการศึกษา พบว่า อัตราส่วนซิลิกาต่ออะลูมินาของซีโอไลต์ชนิด HY และอัตราส่วนของตัวรองรับอะลูมินาต่อซีโอไลต์ชนิด HY มีผลต่อความสามารถในการเร่งปฏิกิริยาคาร์บอนไดออกไซด์รีฟอร์มมิงของมีเทน ในบรรดาตัวเร่งปฏิกิริยาทั้งหมด ซีโอไลต์ชนิด HY ที่มีอัตราส่วนซิลิกาต่ออะลูมินาเป็น 500 ในตัวเร่งปฏิกิริยาโลหะผสมนิกเกิล โคบอลต์บนตัวรองรับผสมอะลูมินา-ซีโอไลต์ชนิด HY ที่มีอัตราส่วนของตัวรองรับ 1:3 แสดงค่าร้อยละการเปลี่ยนแปลงของมีเทนและคาร์บอนไดออกไซด์และค่าร้อยละการเลือกเกิดของไฮโดรเจนสูงสุดและค่าร้อยละการเลือกเกิดของคาร์บอนมอนอกไซด์ต่ำสุด ประสิทธิภาพการเร่งปฏิกิริยาดีที่สุดนั้นเป็นผลมาจากมีการกระจายตัวของโลหะสูงสุด ซึ่งแสดงถึงมีปริมาณโลหะนิกเกิลและโคบอลต์ที่ว่องไวในการทำปฏิกิริยามากที่สุด, ค่าความเป็นกรดต่ำซึ่งนำไปสู่การการดูดซับคาร์บอนไดออกไซด์ที่ดีขึ้น, อุณหภูมิของการรีดิวซ์ต่ำลงซึ่งทำให้มีความสามารถในการรีดิวซ์ของโลหะง่ายขึ้น และมีเสถียรภาพสูงแม้ว่ามีการสะสมตัวของคาร์บอนสูง

ภาควิชา วิศวกรรมเคมี ลายมือชื่อนิสิต .....

สาขาวิชา วิศวกรรมเคมี ลายมือชื่อ อ.ที่ปรึกษาหลัก .....

ปีการศึกษา 2558

5770187221 : MAJOR CHEMICAL ENGINEERING
KEYWORDS: CARBON DIOXIDE REFORMING OF METHANE / NI-CO CATALTST / AL2O3-HY ZEOLITE SUPPORT / SI/AL MOLAR RATIO

TIPANATE CHAOVANICH: Carbon dioxide reforming of methane over Ni-Co catalysts supported on Al_2O_3-HY zeolite. ADVISOR: ASST. PROF. SUPHOT PHATANASRI, D.Eng., 93 pp.

In this research, the effect of Si/Al molar ratios (15, 200 and 500) of HY zeolite in bimetallic Ni-Co over Al_2O_3-HY zeolite catalysts prepared by incipient wetness impregnation method was studied. In addition, the effect of support ratios of Al_2O_3 and selected HY zeolite in bimetallic Ni-Co catalysts was investigated as follows: 3:1, 1:1 and 1:3, and compared to the Al_2O_3 support and HY zeolite support in Ni-Co catalysts. All catalysts were tested in carbon dioxide reforming of methane reaction at 700 °C of reaction temperature under atmospheric pressure and characterized by various techniques. From the results, it was found that Si/Al molar ratios of HY zeolite and support ratio of Al_2O_3 and HY zeolite affect catalytic activity in carbon dioxide reforming of methane, evidenced by characterization results. Among all catalysts, HY zeolite with Si/Al molar ratios of 500 in bimetallic Ni-Co over mixed Al_2O_3-HY500 with a support ratio of 1:3 exhibited the highest CH_4 and CO_2 conversions and H_2 selectivity, and lowest CO selectivity. The best catalytic performance was resulted by the highest metal dispersion which are highest amount of Ni and Co active sites, a lower total acidity leading to greater affinity for CO_2 adsorption, a shift of reduction temperature to lower temperature which are easy reducibility for metal and high stability in spite of highest carbon deposition.

Department:	Chemical Engineering	Student's Signature	.....
Field of Study:	Chemical Engineering	Advisor's Signature	.....
Academic Year:	2015		

ACKNOWLEDGEMENTS

I would like to express my gratefulness and appreciation to my adviser, Assistant Professor Dr. Suphot Phatanasri for his best suggestion, useful discussion and knowledge for this research. This thesis would not have been completed without all the support and guidance that the author have always received from his. In addition, I would also like to thank Associate Professor Dr. Joongjai Panpranot, as the chairman of committee of this thesis, Dr. Chutimon Satirapipathkul and Assistance Professor Dr. Soipatta Soisuwan, as member of committee of this thesis

Most of all, I would like to thank my parents for support, encouragement and suggestion all the time, and to all my friends in Center of Excellence on Catalysis and Catalytic Reaction Engineering for their useful help, advice and encouragement.

Finally, many thanks are given to Thailand Research Fund and Chulalongkorn University for financial support to this work.

CONTENTS

Page

Page

Page

Page

TABLE CONTENTS

Page

FIGURE CONTENTS

Page

CHAPTER I

INTRODUCTION

1.1 Background

Nowadays, world population is rapidly increasing and projected to reach 9.8 billion in 2050. Because of continuously increasing energy consumption that will increase 57% from 2004 to 2030 [1], the depletion of petroleum reserves which is a main resource for energy have been concerned. Moreover, the combustion of fossil fuel releases a large amounts of carbon dioxide. Carbon dioxide is effectively produced by both human and natural source, and remains in the atmosphere. It is the most effective gas causing global warming and greenhouse effect. Greenhouse effect is a natural phenomenon that maintains earth's surface and atmospheric at stable temperature by trapping heat from the sun. Carbon dioxide and methane are the most major greenhouse gases, which have increasing emission, leading to global warming that affects environment. Therefore, many industrial processes have gained an increasing interest in reduction of carbon dioxide and methane emission [2]. A process that has been received many attentions is CO_2 reforming or dry reforming of methane (DRM) (Eq.1.1).

CO_2 reforming or dry reforming of methane (DRM) is the process that converts undesirable greenhouse gases, namely CO_2 and CH_4, into valuable synthesis gases which is a mixture of hydrogen and carbon monoxide [3]. This process is widely used to reduce greenhouse gases emission. Moreover, synthesis gas is used directly for the production of ammonia, methanol, and dimethyl ether and the synthetic fuel alternates through Fischer-Tropsch synthesis [4]. The occurrence of reverse water gas shift (RWGS) (Eq.1.2) influences a syngas.

$CH_4 + CO_2 \leftrightarrow 2CO + 2H_2$ $\Delta H°_{298}$ = 247.3 kJ/mol (Eq.1.1)

$CO_2 + H_2 \leftrightarrow H_2O + CO$ $\Delta H°_{298}$ = 42.1 kJ/mol (Eq.1.2)

Because CO_2 reforming of methane is strong endothermic reaction, it favors at high temperature and heat must be supplied to the process [5]. The major problem of this reaction is catalyst deactivation due to carbon deposition and bed clogging. Deposited carbon is produced through the following side reaction; CH_4 decomposition (Eq.1.3), CO disproportionation or Boudouard (Eq.1.4), and reverse carbon gasification (Eq.1.5). So, catalyst for dry reforming of methane has been interested and developed [6].

$CH_4 \leftrightarrow C + 2H_2$ $\Delta H°_{298}$ = 75.0 kJ/mol (Eq.1.3)

$2CO \leftrightarrow C + CO_2$ $\Delta H°_{298}$ = -172.0 kJ/mol (Eq.1.4)

$CO + H_2 \leftrightarrow C + H_2O$ $\Delta H°_{298}$ = -131.0 kJ/mol (Eq.1.5)

Catalysts that are active for CO_2 reforming of methane are noble metals such as Pt, Rh, and Pd and based metals such as Ni, Co, and Fe. Noble metal catalysts has high activity, excellent stability due to high resistance to carbon deposition compared to Ni-based catalyst but the high cost of noble metals limit available for industrial applications. Therefore, Ni-based catalyst is the most widely used both scientific and industrial for CO_2 reforming of methane. However, it has high sensitive to carbon deposition and sintering at high temperature leading to catalyst deactivation [7]. To overcome the problem, some researches use Ni–Co bimetallic catalysts because of coke formation is reduced by the addition of Co to Ni [8, 9]. In addition, the nature of support influence the activity of DRM. Various support such as Al_2O_3, TiO_2, SiO_2, zeolite and ZrO_2 were used [10, 11]. Among many supports, γ-Al_2O_3 and zeolite have been

interested due to well-defined structure, excellent thermal stability, high surface area and high initial activity of DRM reaction [12]. Type and Si/Al molar ratio of zeolite have different type of acid sites and surface textures which affect metal dispersion, catalytic activity, and coke formation [6, 13, 14].

In this research, the aim is to investigate the effect of Si/Al molar ratio of HY zeolite in bimetallic Ni-Co over Al_2O_3-HY zeolite catalysts, and study the support ratio of Al_2O_3 and HY zeolite. All supports and catalysts were prepared by sol-gel method and incipient wetness impregnation method. The catalysts have been characterized by various techniques, and the catalytic performance and activity for carbon dioxide reforming of methane were investigated.

1.2 Research Objective

1.2.1 To study HY zeolite with different the Si/Al molar ratio in bimetallic Ni-Co over Al_2O_3-HY zeolite catalysts for carbon dioxide reforming of methane.

1.2.2 To investigate the effect of support ratio of Al_2O_3 and selected HY zeolite in bimetallic catalysts on catalytic performance for carbon dioxide reforming of methane.

1.3 Research scope

1.3.1 Preparation of Al_2O_3-HY zeolite support with different Si/Al molar ratio of HY zeolite (15, 200 and 500) by sol-gel method.

1.3.2 Preparation of Al_2O_3, selected HY zeolite from the 1.3.1, and Al_2O_3-selected HY zeolite with ratios of 3:1, 1:1, and 1:3 by sol-gel method.

1.3.3 Preparation of the loading active metal with 5 wt.% of Ni and 5 wt.% of Co on support by incipient wetness impregnation method.

1.3.4 Characterize physical properties of supported nickel catalysts by using various techniques:

- X-ray diffractometry (XRD) to determine crystallite phase.
- Nitrogen physisorption to determine BET specific surface area, pore size and pore volume.
- Ammonia temperature program desorption (NH_3-TPD) to determine acidity of catalysts.
- Hydrogen temperature program reduction (H_2-TPR) to study reducing temperature of the metal oxide.
- Carbon monoxide chemisorption to determine quantities of active site of catalysts and metal dispersion.
- Scanning Electron Microscopy (SEM) to study morphology of catalysts.
- Thermogravimetric analysis (TGA) to study carbon deposition on spent catalyst.

1.3.5 Investigation of the performance of the prepared catalysts for dry reforming of methane reaction under the following condition:

- The prepared catalysts were reduced in flowing H_2 at 500 °C for 1 h prior to reaction with a flow rate of 50 ml/min.
- The mixture of methane and carbon dioxide at an equal molar ratio (1:1) were used as feed with a total flow rate of 60 ml/min.
- The testing of DRM activity of the prepared catalysts were carried out at 700 °C of reaction temperature.
- The composition of reactant and product gases were analyzed by Thermal Conductivity Detector-type gas chromatograph.

1.4 Research methodology

1.4.1 Part I: Comparative HY zeolite with the Si/Al molar ratio of 15, 200, and 500 in bimetallic Ni-Co over Al_2O_3 mixed with HY zeolite catalysts.

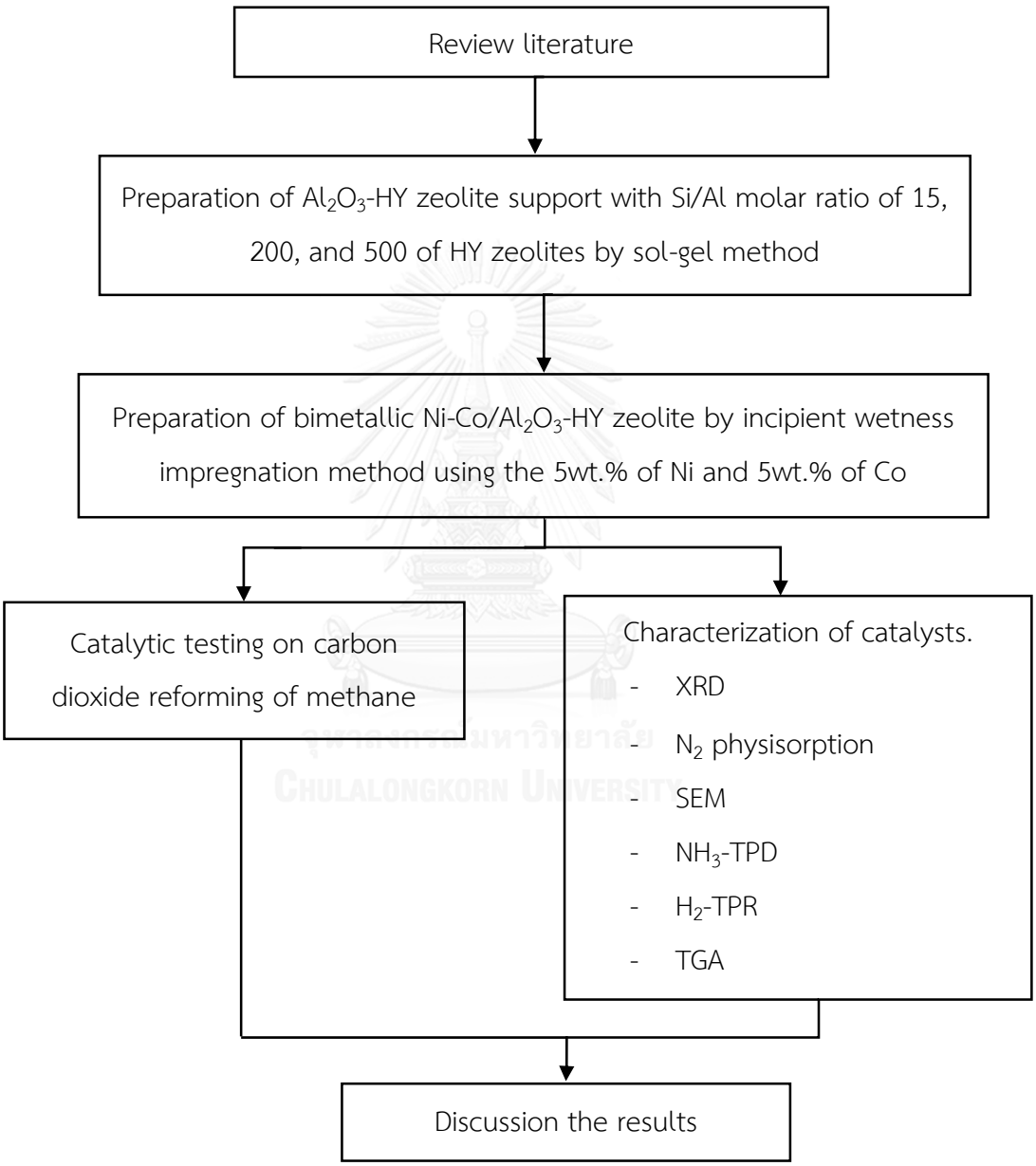

1.4.2 Part II: Investigation the effect of support ratio of Al_2O_3 and selected HY zeolite with ratios of 3:1, 1:1, and 1:3 in bimetallic catalysts.

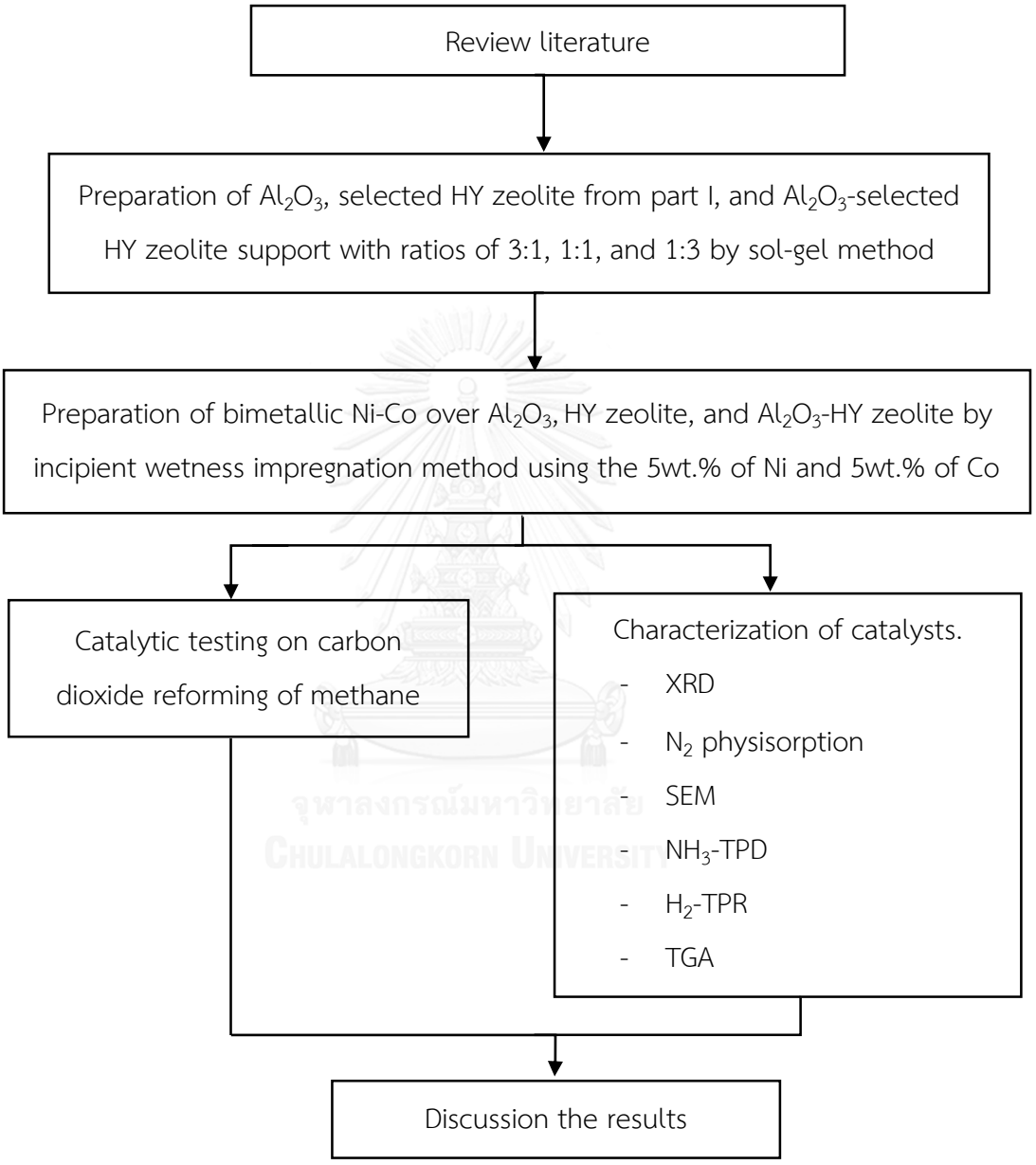

CHAPTER II
THEORY AND LITERATURE REVIEWS

2.1 Synthesis gas and hydrogen production

Hydrogen can be produced from several sources such as biomass, water, hydrocarbon fuels, natural gas, hydrogen sulfide, boron hydrides, and chemical elements with hydrogen [15]. There are many processes for synthesis gas such as through steam reforming, partial oxidation and dry reforming. Each process has different advantages and limitations [16]. Natural gas reforming is also the most economical among all hydrogen production pathways. Hydrogen and synthesis gas can currently be produced from natural gas by means of three different chemical processes:

1) Steam reforming (steam methane reforming or SMR) is the most widespread process. The process uses methane and steam as feedstock, and synthesis gas containing a mixture of hydrogen and carbon monoxide is produced. Steam reforming is operated at a high reaction temperature and pressure because of endothermic reaction [17]. The reaction are also given in Eq.2.1 [18].

$$CH_4 + H_2O \leftrightarrow CO + 3H_2 \qquad \Delta H°_{298} = 206.1 \text{ kJ/mol} \qquad \text{(Eq.2.1)}$$

2) Partial oxidation of natural gas is a process that methane is reacted with oxygen to yield syngas hydrogen and carbon monoxide. The advantage of this process is not a requirement of external heating for reactor because of mildly exothermic reaction. Due to the use of nearly pure O_2, the system requires the separation of

oxygen from air before. This process has higher operating cost than the others reforming process. The partial oxidation reaction is shown in Eq.2.2 [19].

$$CH_4 + 1/2O_2 \leftrightarrow CO + 2H_2 \qquad \Delta H°_{298} = -38 \text{ kJ/mol} \qquad \text{(Eq.2.2)}$$

3) Carbon dioxide reforming of methane (Dry methane reforming or DRM) is a method of producing synthesis gas, which is mixtures of hydrogen and carbon monoxide, from the reaction of carbon dioxide with hydrocarbons such as methane. Synthesis gas is conventionally produced via the steam reforming reaction. In recent years, there are increased concerns on the contribution of greenhouse gases to global warming. Replacing reactant from steam to carbon dioxide is suggested. The dry reforming reaction may be represented by:

$$CH_4 + CO_2 \leftrightarrow 2CO + 2H_2 \qquad \Delta H°_{298} = 247.3 \text{ kJ/mol} \qquad \text{(Eq.2.3)}$$

Thus, two greenhouse gases are consumed and useful chemical building blocks, hydrogen and carbon monoxide, are produced. The reaction equilibrium for production of synthesis gas is typically influenced by reaction of hydrogen with carbon dioxide. The reverse water-gas shift reaction is described by the reaction as follow:

$$CO_2 + H_2 \leftrightarrow H_2O + CO \qquad \Delta H°_{298} = 42.1 \text{ kJ/mol} \qquad \text{(Eq.2.4)}$$

Synthesis as is also used as an intermediate in producing synthetic petroleum for use as a fuel or lubricant via the Fischer–Tropsch process and previously the Mobil methanol to gasoline process. Among the processes, carbon dioxide reforming of methane have gained an increasing interest development because of the utilization of greenhouse gases both hydrocarbon and carbon dioxide [20].

2.2 Carbon dioxide reforming of methane

The carbon dioxide reforming of methane or dry reforming of methane has become interesting processes in many researches and industrials. This reaction consumes the undesirable greenhouse gases, namely carbon dioxide and methane, and produces synthesis gas that consists of hydrogen and carbon monoxide. The synthesis gas is suitable for industrial processes such as methanol, dimethyl ether [4, 21], or useful for liquid hydrocarbons and oxygenates through the well-known Fischer-Tropsch reactions [22]. The advantages of this reaction are as following: (I) it utilizes two major greenhouse gases, (II) the reaction converts undesirable greenhouse gases to valuable synthesis gas, (III) produce hydrogen/carbon monoxide ratio close to 1 that is suitable for synthesis of liquid hydrocarbon. However, the carbon dioxide reforming of methane is favored at high temperature because of highly endothermic reaction. Therefore, this reaction must be operated at high temperature (600-1000 °C), that requires heat to the process, to attain high equilibrium conversion of CH_4 and CO_2 to H_2 and CO and to minimize the thermodynamic driving force for carbon deposition [23].

Table 2.1 The overall reaction for carbon dioxide reforming of methane.

Name	Reaction	ΔH°_{298}
(1) CO_2 reforming of CH_4	$CH_4 + CO_2 \leftrightarrow 2H_2 + 2CO$	247.3 kJ/mol
(2) CH_4 decomposition	$CH_4 \leftrightarrow C + 2H_2$	75.0 kJ/mol
(3) CO disproportionation or Boudouard	$2CO \leftrightarrow C + CO_2$	-172.0 kJ/mol
(4) Reverse water-gas shift	$CO_2 + H_2 \leftrightarrow CO + H_2O$	42.1 kJ/mol
(5) Reverse carbon gasification	$CO + H_2 \leftrightarrow C + H_2O$	-131.0 kJ/mol

The overall reaction for carbon dioxide reforming of methane are shown in Table 2.1. Carbon dioxide reforming of methane (1) produces a synthesis gas with a theoretical hydrogen/carbon monoxide ratio of one. The occurrence of reverse water-gas shift reaction (4) that consumes hydrogen and produce carbon monoxide, occurs hydrogen/carbon monoxide ratio less than one. CH_4 decomposition (2) and CO disproportionation (or Boudouard reaction) (3) generate carbon deposition on surface catalyst, which is a main cause of deactivation of catalyst. CH_4 decomposition and reverse water-gas shift reaction are moderately endothermic reaction, while Boudouard reaction and reverse carbon gasification (5) are exothermic reaction. The conversion of the carbon dioxide reforming of methane increases with increasing reaction temperature because the equilibrium constant of this reaction is highly endothermic reaction. In addition to the conversions, coke deposition is also affected by higher temperatures, which favors methane decomposition and limits the CO disproportionation reaction [24]. Thus, high reaction temperature is more favorable for

the carbon dioxide reforming of methane than the other side reactions. The major drawback of this reaction at high temperature is the sintering of metal particles or support's pores, metal oxidation, or rapid coke deposition which cause catalyst deactivation, catalyst destruction, or reactor blockage. Hence, the catalysts and supports should be appropriately selected to overcome this problem [11].

2.3 Supported catalysts

2.3.1 Alumina

Alumina or aluminium oxide is a chemical compound of aluminium and oxygen with the chemical formula Al_2O_3. It has several names such as aloxide, alundum, or aloxite depend on applications, and several occurring form of aluminium oxide, which aluminium(III) oxide is the most common form. It occurs in nature as the corundum, which form the ruby and sapphire, diaspora, gibbsite, bauxite and many other name.

Alumina is the most common support or employed catalyst in the chemical industry. It has advantages such as its high thermal stability, wide range of chemical and physical properties. The alumina consists of more than a dozen well-characterized amorphous or crystalline structures which vary over wide range of surface area of 0.5-600 m^2/g, pore size, pore size distribution and acidity of surface [25].

Preparation, purity, dehydration, and thermal treatment history influence the crystal structures, physical and chemical properties of alumna. From different crystalline structure, there are many forms of Al_2O_3 such as α, γ, χ, κ, δ, θ, ρ, and η-alumina. Alumina phases, present as a function of temperature, are illustrated in Figure 2.1, and the structure and properties of alumina at different calcination temperature are listed in Table 2.2. The final crystal structure and properties are strongly affected by calcination temperature, treatment and starting matter. By thermal treatment at

high temperature, α-alumina has lowest surface area and acidity of all alumina. γ-alumina is widely used as commercial support and catalyst for industry and laboratory because of its moderately high surface area and stable phase in wide range of reaction temperature [26].

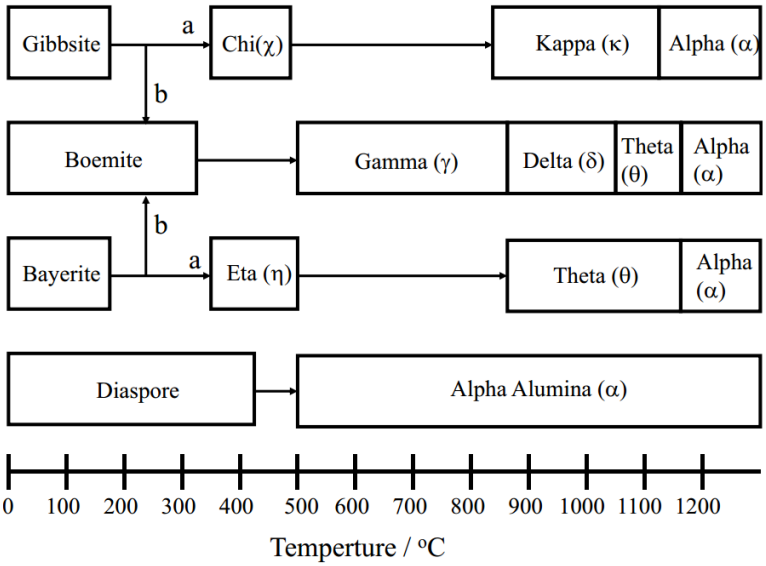

Figure 2.1 Alumina phase present as a function of temperature: (a) corresponds to the path favored for fine crystals, (b) to the path for moist or particles.

Table 2.2 The structure and properties of alumina at different calcination temperature.

Calcination temperature (°C)	Alumina phase	Surface area (m^2/g)	Pore volume (cm^3/g)	Pore diameter (nm)
250	preudoboemite	390	0.50	5.2
450	γ-alumina	335	0.53	6.4
650	γ -alumina	226	0.55	9.8
850	γ -alumina	167	0.58	14
950	δ-alumina	120	0.50	16.6
1050	θ-alumina	50	0.50	28
1200	α-alumina	1-5	-	-

2.3.2 Zeolite (Faujasite)

Zeolites are microporous, hydrated aluminosilicate minerals that are used as ion exchangers, molecular sieves, adsorbents, and catalysts. The name “Zeolite” is derived from Greek, words “Zeo” meaning boil, and words “Lithos” meaning stone. The general formula representing their chemical composition can be written as follows:

$$M_{x/n}(AlO_2)_x(SiO_2)_y.nH_2O$$

From the general formula, M is positive cation with the charge 1, and the y/x ratio represents silicon/aluminium ratio which is importance parameter for zeolite’s properties. Zeolite consists of interlinked tetrahedra of alumina (AlO_4) and silica (SiO_4). In simpler words, they're solids with a relatively open, three-dimensional crystal structure built from the elements aluminum, oxygen, and silicon, with alkali or alkaline-earth metals plus water molecules trapped in the gaps between them. Zeolites form

with many different crystalline structures, which have large open pores or cavities in a very regular arrangement and roughly the same size as small molecules [27].

HY zeolite (Faujasite)

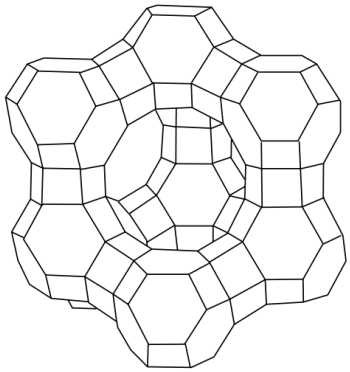

Figure 2.2 Structure of zeolite Y in three-dimensional framework [28].

Zeolite Y, also known as faujasite (FAU) is a framework type of zeolite as shown in Figure 2.2. The naturally occuring zeolite Faujasite consists of linked AlO_4 and SiO_4 tetrahedral. The faujasite framework consists of sodalite cages which are connected through hexagonal prisms. The pores are arranged perpendicular to each other in the x, y, and z planes. The pore, which is formed by a 12-membered ring, has a relatively large diameter of 7.4 Å. The inner cavity has a diameter of 12 Å and is surrounded by 10 sodalite cages. The unit cell is cubic which having lattice constant 24.7 Å [29]. The silica/alumina ratio is one of the parameter that impacts on zeolite's properties such as structure, surface acidity, surface area, and morphology. Zeolite acidity increases in strength as the molar ratio of Si/Al decreases due to the increases in AlO_4^- sites, which strengthens the electro–static field in zeolite and increases the number of acid sites [30]. Zeolite Y has been widely used in industry, especially catalyst, due to well-

defined structure, high potential property, great stability at high temperature, and high affinity for carbon dioxide [12].

2.4 Metal-based catalyst

2.4.1 Nickel metal

Nickel is a transition metal having atomic number 28. The chemical symbol representing nickel is Ni. It is silvery-white, malleable, hard, and ductile metal, and is a member of group VIII of the periodic table. The unit cell of nickel is a face-centered cube (FCC) with the lattice parameter of 0.352 nm, and has an atomic radius of 0.124 nm. Nickel shows a significant chemical activity that can be observed when nickel is powdered to maximize the exposed surface area on which reactions can occur, but larger pieces of the metal are slow to react with air at ambient conditions due to the formation of a protective oxide surface. In compounds of nickel, the oxidation states of nickel are −1, 0, +1, +2, +3, and +4. The +2 state in compounds of nickel is the most common state, having a various compounds of industrial applications such as nickel chloride ($NiCl_2$), nickel nitrate, ($Ni(NO_3)_2.6H_2O$), and nickel sulfate ($NiSO_4$). And more properties of nickel are shown in Table 2.3.

Table 2.3 Properties of nickel [31].

Property	Value
Chemical symbol	Ni
Atomic number	28
Atomic mass	58.6934 g/mol
Phase at room temperature	Solid
Density	8.908 g/cm^3
Melting point	1728 K (1455 °C, 2651 °F)
Boiling point	3003 K (2730 °C, 4946 °F)
Heat of fusion	17.48 kJ/mol
Heat of vaporization	379 kJ/mol
Molar heat capacity	26.07 J/(mol·K)
Oxidation states	4, 3, 2, 1, 0, −1, −2

2.4.2 Cobalt metal

Cobalt is a transition metal having atomic number 27. The chemical symbol representing nickel is Co. Cobalt is a chemical element having silver-white, lustrous, brittle element, and is a hard ferromagnetic metal of group VIIIB of the periodic table. The common oxidation states of cobalt are +2 and +3 states that form a variety of stable compounds with ligands such as water, chloride, and ammonia. These salts form the pink-colored metal aqua complex $[Co(H_2O)_6]^{2+}$ in water. Addition of chloride gives the intensely blue $[CoCl_4]^{2-}$. Cobalt-based catalysts are also important in reactions relate with carbon monoxide. Several reforming reaction such as steam reforming and carbon dioxide reforming, producing hydrogen production, widely uses cobalt oxide-base catalysts to improve activity and stability. Moreover, cobalt is also used as a

catalyst in the Fischer-Tropsch reaction, which used in the hydrogenation of carbon monoxide into liquid fuels. And more properties of cobalt are shown in Table 2.4.

Table 2.4 Properties of cobalt [32].

Property	Value
Chemical symbol	Co
Atomic number	27
Atomic mass	58.933194 g/mol
Phase at room temperature	Solid
Density	8.90 g/cm^3
Melting point	1768 K (1495 °C, 2723 °F)
Boiling point	3200 K (2927 °C, 5301 °F)
Heat of fusion	16.06 kJ/mol
Heat of vaporization	377 kJ/mol
Molar heat capacity	24.81 J/(mol·K)
Oxidation states	5, 4, 3, 2, 1, 0, −1, −2, -3

2.5 Literature reviews

2.5.1 Effect of support catalyst on dry reforming of methane

A. Luengnaruemitchai and A. Kaengsilalai (2008) [33] studied the effect of types of zeolites (zeolite A, zeolite X, zeolite Y, and ZSM-5) and Ni loading (3 wt.%, 5 wt.%, and 7 wt.%) on the catalytic performance of Ni-based catalyst in carbon dioxide reforming of methane. The catalysts were prepared by an incipient wetness impregnation method and then tested in catalytic activity at 700 °C. The result found that Ni/zeolite Y exhibited better catalytic performance than the other types of studies zeolite because of low amount of Lewis acid sites. The stability of the Ni/zeolite Y was improved with the deactivation of catalyst not observed. A weight of Ni loading at 7 wt.% was the optimum value for each zeolite support but produced a higher amount of coke deposition on the catalyst than the others.

S. Talkhoncheh and M. Haghighi (2015) [34] studied the influence of types of supports on catalytic performance in dry reforming of methane. Ni-based nanocatalysts over clinoptilolite, ceria, and alumina were prepared by impregnation method. The result showed that Ni/Al_2O_3 occurred the highest conversion, yield, and stability. Ni/CeO_2 had well dispersion of Ni species while Ni/Al_2O_3 had high specific area and homogenous distributions. Therefore, the different supports affected catalyst's structure, metal dispersion, distribution, and catalytic activity.

R. Alotaibi et al. (2015) [13] evaluated two different zeolites-type Y in term Si/Al ratio (5.1 and 12) and the effect of promoter (lanthanum and calcium) in Ni-based catalysts on dry reforming of methane. The catalysts were synthesized by incipient wetness impregnation method, and fixed at 10 wt.% of active metal and 10 wt.% of

promoter. From the result, Ca promoted on Ni/zeolite Y (5.1) showed the higher activities than catalysts supported on zeolite Y (5.1), but gave less time on stream stability. This implied that addition of Ca may change the interaction between the zeolite and the Ni particles. In zeolite Y (12), La-containing catalyst occurred more stability with a less carbon deposition on catalyst because addition of La influence the acidity of catalyst. Compared two different zeolite Y, the result revealed that zeolite Y (5.1) had the higher conversion of CH_4 and CO_2 than zeolite Y (12). This implied that increasing of Si/Al molar ratio improved catalytic activity. They concluded that different Si/Al molar ratio of zeolite had different types of acid sites and surface structure.

B. Sarkar et al. (2012) [35] synthesized nanoparticle Ni over mesoporous ZSM-5 support by dispersing colloidal Ni over support with varying Ni loading. ZSM-5 was used as support because of high surface area and thermal stability, and was prepared by hydrothermal method. The activity was tested on reforming of methane with carbon dioxide at different temperatures (650-900 °C). The H_2-TPR profiles for Ni/ZSM-5 showed two reduction peaks at 617 °C and 793 °C, indicating two different reduction of Ni^{2+} species sites to metal Ni on ZSM-5. The first peak at 617 °C is ascribed to Ni nanoparticles outside the mesoporous ZSM-5 while the higher temperature peak at 793°C is attributed to reduction of highly dispersed nanoparticle Ni inside mesopore of ZSM-5. The conversion of this catalysts was higher in comparison with Ni over physical mixing of SiO_2 and Al_2O_3, and Ni over H-ZSM-5. It should be considered that the decreasing activity is due to weak adsorption of CO_2 with the acidic support. The 5%Ni loaded catalyst showed the best activity and stability at reaction temperature of 800 °C. In addition, the deactivation of catalyst may be due to deposited carbon and formation of $NiCO_3$ on catalyst.

M. Inaba et al. (2002) [14] investigated nickel supported on USY, H-ZSM-5, H-Mordenite and H-Beta zeolites with different Si/Al_2 molar ratio, and SiO_2 (Cab-O-Sil) for methane decomposition. The catalysts were prepared by impregnation method and characterized by N_2-adsorption, TG, XRD, SEM, and NH_3-TPD. NH_3-TPD and TG analysis were observed that the amount of desorbed ammonia from catalyst was inversely proportional to the values of carbon deposition, it was suggested that less amount of desorbed ammonia, relating higher Si/Al_2 molar ratio of zeolite, leaded to longer life time of catalyst. The deposited carbon was not affect to surface area, pore volume, and pore diameter indicating that only outer surface area effects on the catalytic activity. In addition, Ni supported on USY type zeolites with Si/Al_2 molar ratio of 14.0 and 360 were found to have higher activity and longer catalytic lifetime than the others.

H. Inoue et al. (2002) [36] compared a conventional Ni/Al_2O_3, Ni/zeolite with different type of zeolites (H-Y, H-mordenite, and Na-mordenite), and Ni over mixed support between Al_2O_3 and zeolite (1:1 weight ratio) that were prepared by impregnation method. The reforming of methane with carbon dioxide was carried out at 750 °C. They reported that Ni/Al_2O_3 showed lower initial conversion and increased within 24 h, while Ni/Al_2O_3-zeolite showed higher conversion and also remained stable. This could be attributed to the formation of $NiAl_2O_4$ from calcination of $Ni(NO_3)_2/Al_2O_3$ at 400 °C. Among mixed support between Al_2O_3 and zeolite, Ni/Al_2O_3-H-mordenite has the highest activity and stability. Differential curves of the TPO of all catalysts had two peaks, one at the lower temperature assigned to the desorption of adsorbed small molecules, the other relating to the oxidation of carbon on surface catalysts. In summary, Ni over Al_2O_3-H-mordenite with composition of Al_2O_3 and H-mordenite 1:1 exhibited best catalytic performance for DRM.

2.5.2 Effect of metal catalyst on dry reforming of methane

M. Sharifi et al. (2015) [37] synthesized bimetallic Ni-Co over zeolite Y for the production of synthesis gas via carbon dioxide reforming of methane. This research compared zeolite Y and Ni-Co over zeolite Y, and optimized composition of Ni-Co bimetallic catalysts that were prepared by sonochemical method. They reported 7 wt.% Ni-3 wt.% Co showed the highest reactants conversion and products yield, and also remained stable during 10 h without deactivation of catalyst. The characterizations of this catalyst displayed smaller particles size and more uniform distribution than others.

D. San-Jose´-Alonso et al. (2009) [9] compared monometallic Ni, Co and bimetallic Ni-Co supported alumina catalyst with 9 wt.% nominal metal content in dry reforming of methane. All catalysts were prepared by excess volume impregnation and pretreated in N_2. The activities were testing at 700 °C, which avoids Co oxidation leading to deactivation. The results found that Co(9) and Ni-Co(1–8) catalysts has high activity and excellent stability in comparison with the others. The remarkable stability of the Co rich catalysts seems to be related with the presence of large particles that are involved in long-term conversion. This implied that Co rich catalysts improved catalytic performance. However, Co rich catalysts generated a large amount of carbon deposition that produced by methane decomposition. Carbon that deposited on catalysts could be ascribed to filamentous carbon. Hence, Co rich catalysts could be used to improve catalytic performance for synthesis gas production.

I. Luisetto et al. (2012) [8] investigated monometallic Co and Ni, and bimetallic Co-Ni over ceria in dry-methane reforming. All catalysts were synthesized by surfactant

assisted co-precipitation method. The content of active phase in both monometallic and bimetallic system is 7.5 wt.%. Catalytic performance, both activity and stability, were tested under atmospheric pressure as function of temperature and time on stream with equimolar mixture of CO_2 and CH_4. From the results, 3.75 wt.% of Co and 3.75 wt.% of Ni in bimetallic catalyst showed better both conversions and H_2/CO ratio than the other monometallic catalysts, which are consistent with H_2-TPR results having the Co-Ni alloy peak at high temperature. They reported that the turnover frequency was greater in Co-Ni/CeO_2 than the others. This could be attributed that Co-Ni alloy is active phase for this reaction. TG result revealed that Co-containing catalysts had lower amounts of carbon deposition in comparison with Ni monometallic system, indicating that having Co in catalyst enhanced the resistance to carbon deposition. So, bimetallic Co-Ni over ceria can be effective catalyst for dry-methane reforming.

S. Sengupta et al. (2014) [38] applied nickel, cobalt, and nickel-cobalt supported alumina on the reforming of methane with carbon dioxide (DRM) and methane cracking reactions. The catalysts were prepared by incipient wetness impregnation method containing 15 wt.% of total metal with varying content of nickel-cobalt in bimetallic system. The results from DRM reaction showed that bimetallic nickel-cobalt supported alumina had better conversions and product hydrogen/carbon monoxide ratio than monometallic catalysts. The initial TOF_{DRM} for Ni-Co catalysts had higher than Ni supported alumina, and the highest average TOF_{DRM} was achieved by Ni-Co catalyst, having Ni:Co ratio of 3:1 (75Ni25Co/Al_2O_3). This suggested that the Ni-Co alloys sites had higher activity than the Ni sites. The maximum amount of carbons (0.2 g/g_{cat}) were deposited on 75Ni25Co/Al_2O_3 catalyst, corresponding to the highest activity.

H. In et al. (2014) [39] studied the effect of Ni/γ-Al2O3, Co-Ni/γ-Al2O3, and Mg-Co-Ni/γ-Al2O3 catalysts on coke formation for carbon dioxide reforming of methane. The stability and activity of catalysts decreases in the following order: 3Mg3Co3Ni > 3Co3Ni > 6Ni. The addition of MgO on catalyst affects accelerating decomposition or dissociation of CH_4 and CO_2. The 3Mg3Co3Ni catalyst produces amorphous carbon deposited, which is easily oxidized, and inhibits a fatal encapsulating type carbon leading to catalyst deactivation, confirming the good stable activity of catalyst for the addition of MgO. So, the addition of Co and MgO has potentially high carbon resistance.

J. Estephane et al. (2015) [40] prepared monometallic and bimetallic Ni and/or Co on ZSM-5 support by wet impregnation method, and studied aging and carbon deposition with varying the metal loading. They reported that carbon deposition forms a passivating layer preventing the re-oxidation of catalyst. The presence of Co prevents catalyst deactivation by oxidation of carbon particle and soot. The higher content of Co causes effectively a decrease in amount of deposited carbon. Hence, Co acted as a synergist to Ni for CRM. Moreover, they was conclude that carbon deposition is highly dependent on active phase content and reaction temperature.

CHAPTER III
EXPERIMENTAL

This chapter describes about the experimental procedures which consists of 3 sections. First, supports and catalysts were prepared. Second, catalysts were characterized by various techniques. Finally, the carbon dioxide reforming of methane was studied and analyzed by Thermal Conductivity Detector-type gas chromatograph.

3.1 The preparation of supports and catalysts

The chemicals that were used for the preparation of supports and catalysts are listed in Table 3.1.

Table 3.1 The chemicals for the preparation of supports and catalysts.

Chemical	Supplier
Alumina isoproproxide (>98%)	Aldrich
HY zeolite (Si/Al molar ratio = 15)	TOSOH
HY zeolite (Si/Al molar ratio = 200)	TOSOH
HY zeolite (Si/Al molar ratio = 500)	TOSOH
Ethanol (99%)	Merck
Hydrochloric acid (37.7 %)	RCI Labscan
Nickel (II) nitrate hexahydrate (98%)	Aldrich
Cobalt (II) nitrate hexahydrate (98%)	Carlo Erba

3.1.1 The preparation of Al_2O_3 supports by sol-gel method

The Al_2O_3 as supports were prepared by sol-gel method. Alumina isoproproxide and ethanol were used as Al_2O_3 precursor and organic solvent, respectively. Alumina isoproproxide was first dissolved in a mixture of deionized water and ethanol with volume ratio of 1:1 by mild stirring at 80 ºC for 1 h. Subsequently, increased the temperature of solution to 90 ºC. After that, hydrochloric acid was dropped to adjust pH value of the solution equal to 2.5 and aged with stirring at 90 ºC, until eliminating solvent. After this step the sol was became so viscous. The formed gel was dried overnight at 110 ºC and calcined under air flow at 550 ºC for 2 h.

3.1.2 The preparation of Al_2O_3-HY zeolite supports by sol-gel method

The Al_2O_3-HY zeolite as supports were prepared by sol-gel method. Alumina isoproproxide and ethanol were used as Al_2O_3 precursor and organic solvent, respectively. Alumina isoproproxide was first dissolved in a mixture of deionized water and ethanol with volume ratio of 1:1 by mild stirring at 80 ºC for 1 h. Subsequently, increased the temperature of solution to 90 ºC and then added HY zeolite (Si/Al molar ratio = 15, 200 and 500) with varied compositions (Al_2O_3/HY zeolite weight ratio 1:3, 1:1 and 3:1) into the solution. After that, hydrochloric acid was dropped to adjust pH value of the solution equal to 2.5 and aged with stirring at 90 ºC, until eliminating solvent. After this step the sol was became so viscous. The formed gel was dried overnight at 110 ºC and calcined under air flow at 550 ºC for 2 h.

3.1.3 The preparation of catalysts by the incipient wetness impregnation method

The bimetallic nickel-cobalt catalysts were prepared by the incipient wetness impregnation method using $Ni(NO_3)_2.6H_2O$ and $Co(NO_3)_2.6H_2O$ as metal precursors with nickel loading of 5 wt.% and cobalt loading of 5 wt.%. First of all, $Ni(NO_3)_2.6H_2O$ and $Co(NO_3)_2.6H_2O$ were dissolved in deionized water in equal volume to pore volume of the support. An aqueous solution of $Ni(NO_3)_2.6H_2O$ and $Co(NO_3)_2.6H_2O$ was dropped to the support. After that, the impregnated catalysts were kept at room temperature for 4 h to assure adequate distribution of metal complete. Finally, the catalysts were dried overnight at 110 ºC and calcined under air flow at 500 ºC for 2 h.

3.2 Catalyst characterization

3.2.1 X-Ray diffraction (XRD)

X-ray diffraction (XRD) analysis were characterized to determine the crystallite phase of the support and catalyst by using X-ray diffractometer SIEMENS D 5000. It was connected to a personal computer with Diffract AT version 3.3 program for fully control of XRD analyzer. The XRD analysis was conducted to Cu-Kα radiation between 20º and 80º with a generator voltage and current of 30 kV and 30 mA, respectively. The scan step was 0.04º.

3.2.2 Nitrogen physisorption

Brunauer–Emmett–Teller (BET) method is used to determine specific surface area of the catalysts, and Barret-Joyner-Halenda (BJH) method is used to examine pore diameter and pore volume of the prepared catalysts. 0.1 grams of each samples were measured by N_2 adsorption-desorption isotherm using Micromeritics ASAP 2020 at

liquid nitrogen temperature of -196 ºC. Prior to the analysis, samples were dried to eliminate moisture in the sample.

3.2.3 Scanning Electron Microscope (SEM)

Scanning electron microscope (SEM) is most widely used to study morphology structure and agglomeration of the sample particles. The sample were analyzed by JEOL mode JSM-5800LV of scanning electron microscopy technique.

3.2.4 Thermogravimetric analysis (TGA)

The as-spun alumina fibers was subjected to the thermogravimetric analysis (Diamond Thermogravimetric and Differential Analyzer, TA Instruments SDT Q600) to determine the carbon content in the sample, as well as their thermal behaviors in the range of room temperature to 1000 ºC. The analysis was performed at a heating rate of 10 ºC /min in 100 ml/min flow of air.

3.2.5 Hydrogen Temperature Programmed Reduction (H_2-TPR)

Temperature Programmed Reduction of Hydrogen (H_2-TPR) analysis was used to evaluate the reducing temperatures of prepared catalysts by using Micromeritics chemisorp 2750 Pulse Chemisorption System. 0.1g of the sample was conducted in a quartz U-tube and pretreated with 25 mL/min of nitrogen flow at 500 ºC for 1 h. The sample was heated with 25 mL/min of 10%H_2 in Ar mixture gas flow from 30 ºC to 800 ºC. The H_2 uptake amount was measured as a function of temperature using TCD.

3.2.6 Ammonia Temperature Programmed Desorption (NH_3-TPD)

The acid properties of catalysts were observed by Ammonia Temperature Programmed Desorption (NH_3-TPD) using Micromeritics chemisorp 2750 Pulse Chemisorption System. 0.1 g of the sample was conducted in a quartz U-tube and pretreated in a helium flow at 500 ºC for 1 h and then ammonia was introduced with helium about 30 min. The sample was heated from 40 ºC to 550 ºC with a heating rate of 10 ºC/min. The desorbed ammonia was measured as a function of temperature using TCD.

3.2.7 CO chemisorption

CO chemisorption analysis was used to evaluate the amount of metal active sites and the metal dispersion of prepared catalysts by using Micrometritics Chemisorb 2750 and ASAP 2101CV.3.00 software unit fitted with a Thermal Conductivity Detector (TCD). Approximately 0.05 g of the sample was conducted in a glass U-tube and purged the sample with helium around 5 min in order to remove remaining air. The sample were reduced with 25 mL/min of hydrogen flow at 500 ºC for 1 h, and then cooled down temperature to 30 ºC that is adsorbed temperature of CO. After that, 20 μL of CO was pulsed over reduced sample at 30 ºC and repeated until the desorption peaks were constant. The amount of metal active sites and percentages of metal dispersion were calculated based on the assumption that only CO molecule is adsorbed on one metal site.

3.3 Catalyst performance test in carbon dioxide reforming of methane

3.3.1 Gas materials for reaction

Gas materials that were used for the catalytic testing are listed in Table 3.2.

Table 3.2 Gas materials that were used for the catalytic testing.

Gas materials or reagent	Supplier
Methane in Carbon dioxide (50%)	The Linde group
Ultra high purity grade nitrogen (99.999%)	Thai industrial Gases Limited
Ultra high purity grade hydrogen (99.999%)	Thai industrial Gases Limited

3.3.2 Instrument and apparatus

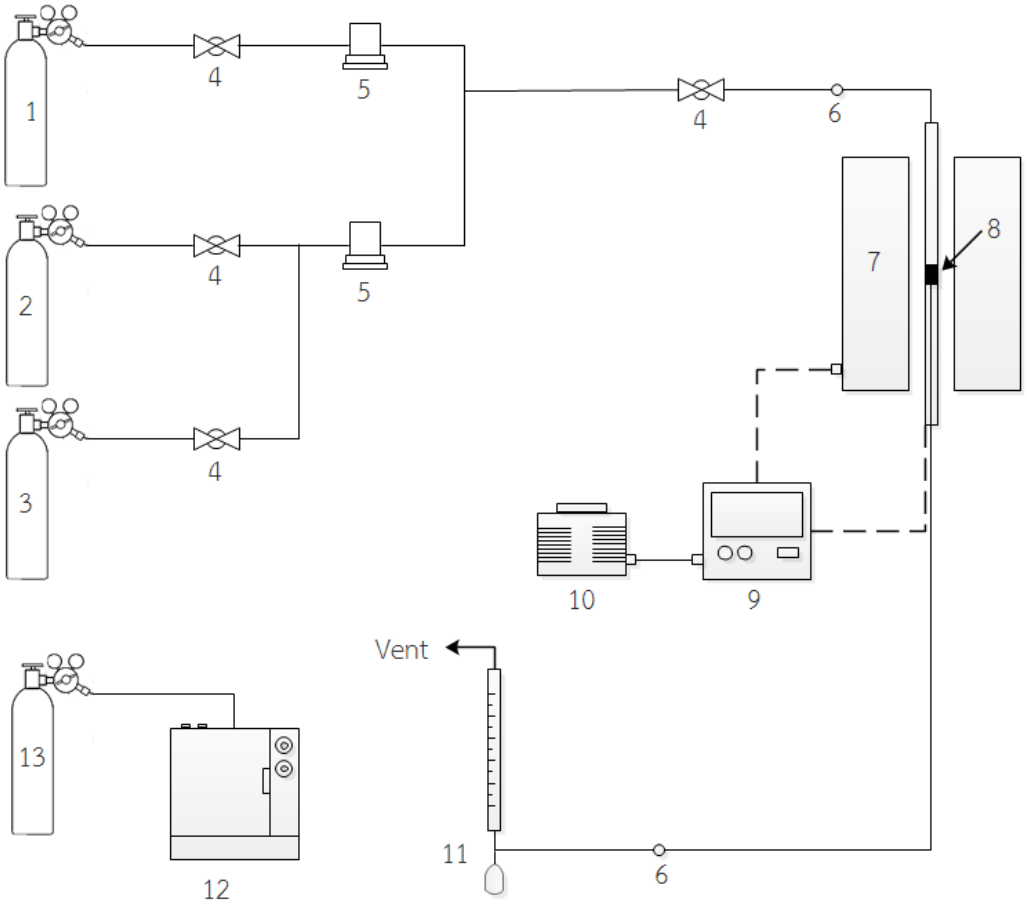

Figure 3.1 Scheme diagram of carbon dioxide reforming of methane reaction.

1. 50% CH_4 in CO_2 cylindrical tank
2. N_2 cylindrical tank
3. H_2 cylindrical tank
4. On-Off valve
5. Mass flow meter
6. Sampling
7. Furnace
8. Quartz tube
9. Temperature controller
10. Variable voltage transformer
11. Bubble flow meter
12. GC-TCD
13. Ar cylindrical tank

Reactor

The reactor is a fixed-bed continuous-flow reactor made from a quartz tube with length of 47.0 mm. and inner diameter of 9.0 mm. The catalysts were packed on quartz wool layers.

Automatic Temperature and Controller

There is a magnetic switch connected to a variable voltage transformer and a temperature controller connected to a thermocouple attached to the catalyst bed in reactor. A dial setting established a set point at any temperature within the range between 0°C to 1000°C

Electric Furnace

This supply the required heated to the reactor for reaction. The reactor could be operating at 700°C.

Gas Controlling Systems

Gas was controlled by pressure regulator (0-120 psig). On-off valve and needle valve were used to adjust flow rate of gas.

Gas Chromatographs

The composition of inlet and exit gas were analyzed by Thermal Conductivity Detector-type gas chromatograph (Shimudzu, GC-8A) equipped Operating conditions are shown in Table 3.3.

Table 3.3 Operating conditions of gas chromatographs.

Gas Chromatograph	**Shimudzu, GC-8A**	
Detector	TCD	TCD
Column	Porapack-Q	Molecular sieve 5A
Carrier gas	Argon	Argon
Carrier gas flow	50 ml/min	50 ml/min
Column temperature		
- Initial	70 °C	70 °C
- Final	70 °C	70 °C
Detector temperature	100 °C	100 °C
Injector temperature	100 °C	100 °C
Current	80 mA	80 mA
Analyzed gas	CO_2	H_2, CH_4, CO

3.3.3 Reaction method

Carbon dioxide reforming of methane was carried out in a fixed-bed continuous-flow quartz reactor. The reactor temperature was measured and controlled by K-type thermocouple positioned at the middle of catalyst bed. The 0.05 g of prepared catalyst was conducted into the reactor and reduced in flowing hydrogen at 500 °C for 1 h prior to reaction with a flow rate of 50 ml/min. Nitrogen was purged to replace hydrogen with a flow rate of 50 ml/min, and the catalyst was heated to the reaction temperature with a heating rate 10 °C/min. The catalytic performance was tested at 700 °C for 3 h using the feed volume ratio of CH_4:CO_2 = 1:1 with a total feed flow rate of 60 ml/min. The composition of feed and product gas was analyzed by

Thermal Conductivity Detector-type gas chromatograph (Shimudzu, GC-8A) equipped with Porapak-Q and Molecular sieve 5A packed column using argon as carrier gas with a flow rate of 30 mi/min.

CHAPTER IV
Results and discussion

In this chapter consists of two parts. The first part studies the effect of different Si/Al molar ratio of HY zeolite (15, 200 and 500) on Ni-Co over Al_2O_3-HY zeolite catalysts. The second part investigates the effect of support ratio of Al_2O_3 and selected HY zeolite on catalysts, and compare to the Al_2O_3 support and HY zeolite support in bimetallic catalysts. Support ratio of Al_2O_3 and selected HY zeolite are as follows: 3:1, 1:1, 1:3. Each part shows the characterization of catalysts by X-Ray diffraction pattern (XRD), Nitrogen adsorption-desorption, Scanning Electron Microscopy (SEM), Ammonia temperature program desorption (NH_3-TPD), Hydrogen temperature programmed reduction (H_2-TPR), Carbon monoxide chemisorption, Thermo gravimetric analysis (TGA), and activity in carbon dioxide reforming of methane.

4.1 The effect of different Si/Al molar ratio of HY zeolite (15, 200 and 500) in Ni-Co over Al_2O_3-HY zeolite catalysts.

The catalyst nomenclatures are represent as below:

Ni-Co/Al_2O_3-HY15 represents the catalyst which have Ni and Co over Al_2O_3-HY zeolite support with HY zeolite having Si/Al molar ratio of 15.

Ni-Co/Al_2O_3-HY200 represents the catalyst which have Ni and Co over Al_2O_3-HY zeolite support with HY zeolite having Si/Al molar ratio of 200.

Ni-Co/Al_2O_3-HY500 represents the catalyst which have Ni and Co over Al_2O_3-HY zeolite support with HY zeolite having Si/Al molar ratio of 500.

4.1.1 Catalyst characterization

4.1.1.1 X-Ray diffraction pattern (XRD)

The X-ray diffraction (XRD) patterns of Al_2O_3-HY zeolite supports with different Si/Al molar ratios of HY zeolites (HY15, HY200 and HY500) are shown in Figure 4.1. XRD was performed regarding the crystallite phases of the samples. Al_2O_3 crystalline phase were obvious at 2θ = 37.2° and 45.9°, and the XRD patterns of HY zeolite were obvious at 2θ = 20.3°, 23.7°, 27.0°, 31.8°, 34.2°, 38.4° and 54.6° for all Si/Al molar ratios which are typical of alumina and zeolite faujasite, respectively [41]. The mixed alumina and HY zeolite for all Si/Al molar ratio of zeolites had similar pattern to alumina and zeolite faujasite [42]. It is seen that Si/Al molar ratios of HY zeolite did not affect crystallite phases of the support

The XRD patterns of the bimetallic Ni-Co over Al_2O_3-HY zeolite catalysts with Si/Al molar ratios = 15, 200, and 500 are shown in Figure 4.2. Although all XRD patterns were dominated by the support peaks, there are diffraction peaks at 2θ = 43.5° and 64.5° corresponding to nickel oxide and/or nickel aluminate, and diffraction peaks at 2θ = 36.9°, 43.5°, 59.4° and 64.5° corresponding to cobalt oxide and/or cobalt aluminate [43]. Diffraction peak of Al_2O_3-HY zeolite support in bimetallic catalysts did not change indicating no phase transformation during incipient wetness impregnation [44].

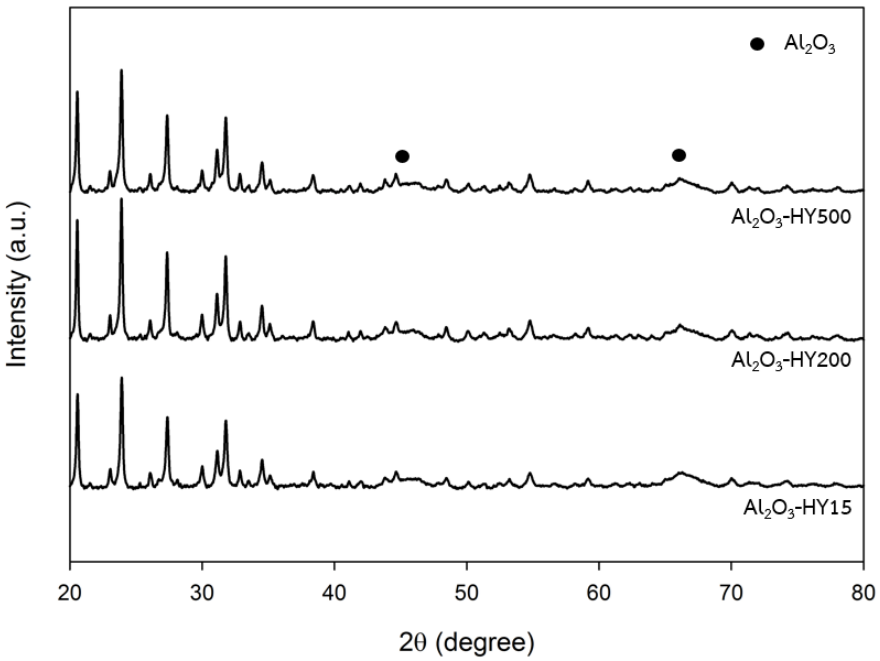

Figure 4.1 XRD patterns of Al_2O_3-HY zeolite with different Si/Al molar ratio of zeolites.

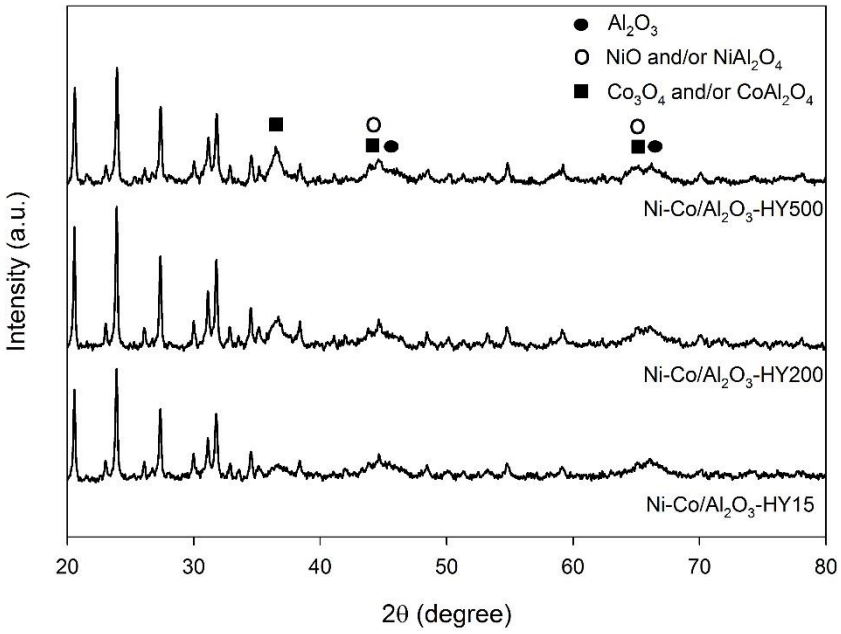

Figure 4.2 XRD patterns of Ni-Co over Al_2O_3-HY zeolite catalysts with different Si/Al molar ratio of zeolites.

4.1.1.2 Nitrogen adsorption-desorption

The textural properties of support and catalysts were investigated by nitrogen adsorption-desorption technique using Brunauer–Emmett–Teller (BET) method and Barret-Joyner-Halenda (BJH) method. The BET surface area, pore volume and pore size were summarized in Table 4.1. The BET surface area of alumina-HY zeolite supports were ranged between 455-516 m^2/g, while the BET surface area of Ni-Co/ Al_2O_3-HY zeolite catalysts were ranged between 370-427 m^2/g. The BET surface area of catalysts were decreased compare to the supports. This suggests that the metal can access to the pores of support, so that the pore may be blocked by the metal [45]. The pore volume of supports and catalysts were range 0.21-0.34 cm^3/g. The pore volume of supports were lower than catalysts due to nickel and cobalt metal may block the pore of catalysts [46]. The pore size of supports and catalysts were range 4.9-5.2 nm that it had no significant change.

Table 4.1 The physiochemical properties of supports and catalysts with different Si/Al molar ratio of HY zeolites.

Catalysts	BET surface area (m^2/g)	Pore volume (cm^3/g)	Pore size (nm)
Al_2O_3-HY15	455	0.28	5.0
Al_2O_3-HY200	516	0.34	5.1
Al_2O_3-HY500	502	0.31	5.2
Ni-Co/Al_2O_3-HY15	370	0.21	4.9
Ni-Co/Al_2O_3-HY200	427	0.25	5.1
Ni-Co/Al_2O_3-HY500	414	0.24	5.2

The N_2 adsorption-desorption isotherm for Al_2O_3-HY zeolites support and Ni-Co/Al_2O_3-HY zeolite catalysts with different Si/Al molar ratios of HY zeolites are displayed in Figure 4.3 and Figure 4.4, respectively. The isotherms of both supports and catalysts can be classified as a type IV isotherm with H3-shaped hysteresis loops that are implied micro-mesoporous structure [47].

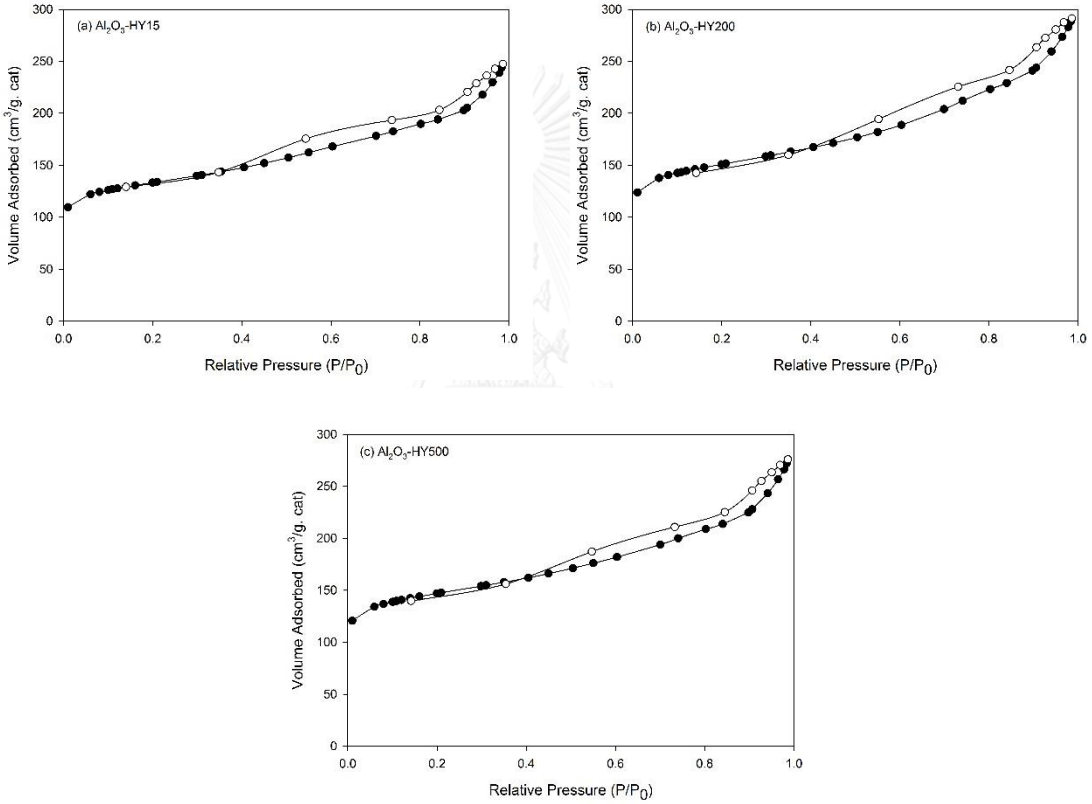

Figure 4.3 N_2 adsorption-desorption isotherm of Al_2O_3-HY zeolite support with different Si/Al molar ratio of HY zeolites.

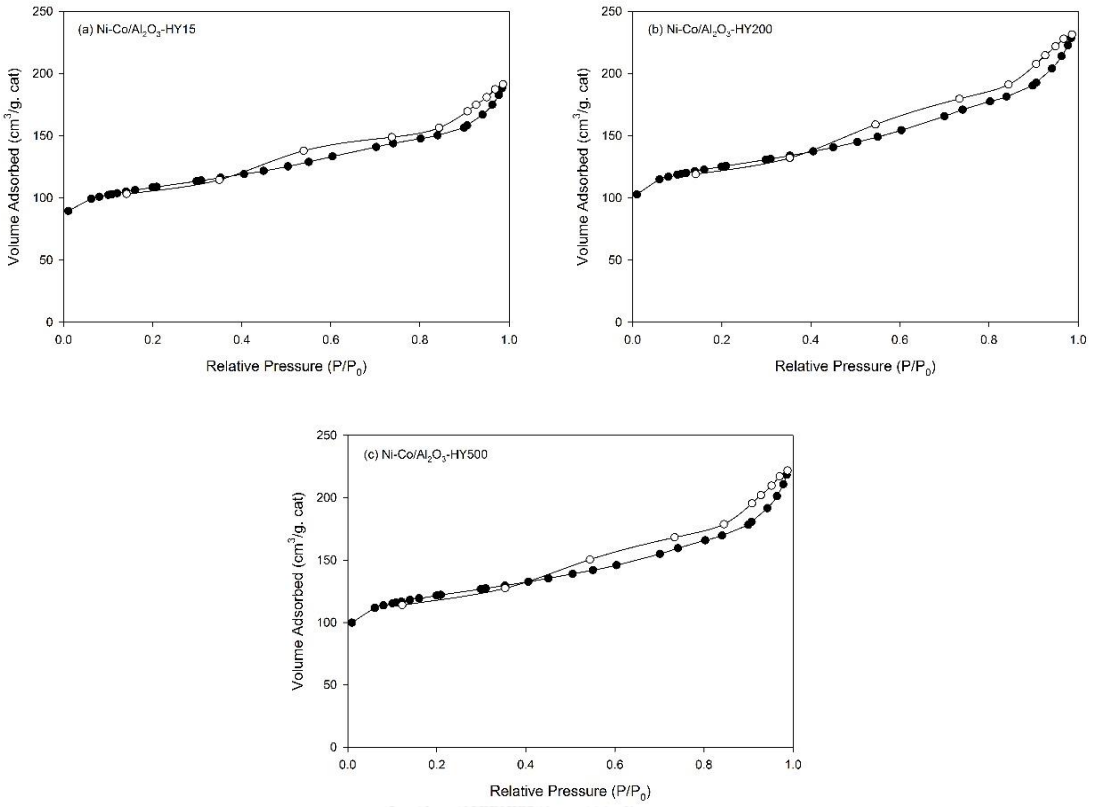

Figure 4.4 N_2 adsorption-desorption isotherm Ni-Co/Al_2O_3-HY zeolite catalysts with different Si/Al molar ratio of HY zeolites.

4.1.1.3 Hydrogen temperature programmed reduction (H_2-TPR)

Hydrogen temperature programmed reduction (H_2-TPR) was used for investigating the reduction behavior of the samples. Metal, support and metal-support interaction affect the H_2-TPR profiles, resulting different the reducibility and reduction temperature of catalysts. The H_2-TPR profiles of Ni-Co/Al_2O_3-HY zeolite catalysts with different Si/Al molar ratios (HY15, HY200 and HY500) are demonstrated in Figure 4.5. From the previous work, the reducibility of NiO particle in Ni-based catalyst possess one peak which was attributed to reduction from NiO to Ni species [38], while Co-based catalysts shown two peaks which were attributed to reduction from Co_3O_4 to CoO species and reduction from CoO to Co species [48]. According to H_2-TPR profiles

of catalysts, it was obvious that bimetallic Ni-Co catalysts exhibited two reduction peaks. The first peak of Ni-Co/Al_2O_3-HY15, Ni-Co/Al_2O_3-HY200 and Ni-Co/Al_2O_3-HY500 were related to the reduction from Co_3O_4 to CoO species, which were observed at 331 °C, 347 °C and 337 °C, respectively. The second peak was represented to reduction from NiO to Ni and CoO to Co metallic that was located at 440 °C, 484 °C and 443 °C for HY15, HY200 and HY500 in catalysts, respectively. Ni-Co/Al_2O_3-HY500 had higher intensity of peaks than the others. This is indicated that it was easier reducibility in Ni-Co/Al_2O_3-HY500 [49].

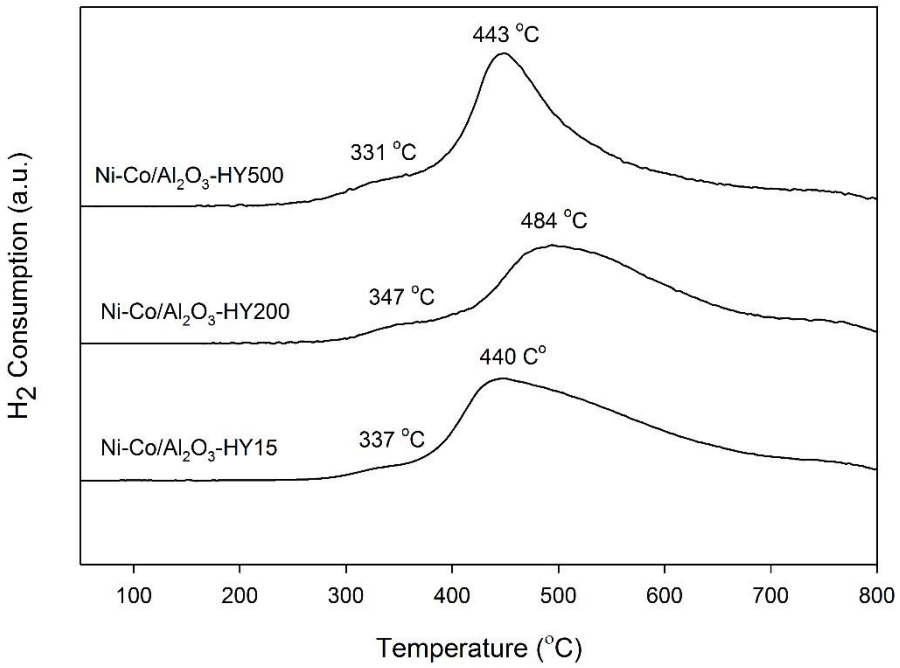

Figure 4.5 H_2-TPR profiles of Ni-Co/Al_2O_3-HY zeolite catalysts with different Si/Al molar ratio of HY zeolites (HY15, HY200 and HY500).

4.1.1.4 Ammonia temperature program desorption (NH_3-TPD)

The acidity on surface of the catalysts with different Si/Al molar ratio of HY zeolites were determined by ammonia temperature program desorption (NH_3-TPD). The amount of desorbed ammonia relates to the total surface acidity of the catalysts, and the desorption temperature of desorbed ammonia corresponds to the acid strength on surface of the catalysts [50].

The NH_3 desorption curves as a function of the temperature of the Ni-Co/Al_2O_3-HY zeolite catalysts with different Si/Al molar ratio of HY zeolites (HY15, HY200 and HY500) are shown in Figure 4.6. Ni-Co/Al_2O_3-HY15, Ni-Co/Al_2O_3-HY200 and Ni-Co/Al_2O_3-HY500 exhibited only one desorption peak at low desorption temperature indicating the presence of weak acid sites [51]. In addition, peaks were decreased with an increase Si/Al molar ratio of HY zeolites (from HY15 to HY500), which corresponds to the total surface acidity of the catalysts [52]. Table 4.2 shows the total acidity of Ni-Co/Al_2O_3-HY zeolite catalysts with different Si/Al molar ratios of HY zeolites. The total acid sites of Ni-Co/Al_2O_3-HY15, Ni-Co/Al_2O_3-HY200 and Ni-Co/Al_2O_3-HY500 were ranged between 9.53-14.58 mmol NH_3/g.cat. Ni-Co/Al_2O_3-HY15 exhibited highest total acidity. This result indicated that the total acid sites of samples decreased with increasing of Si/Al molar ratio of HY zeolite. However, the higher acidity may hamper CO_2 adsorption and activation led to lower catalytic activity [13, 53].

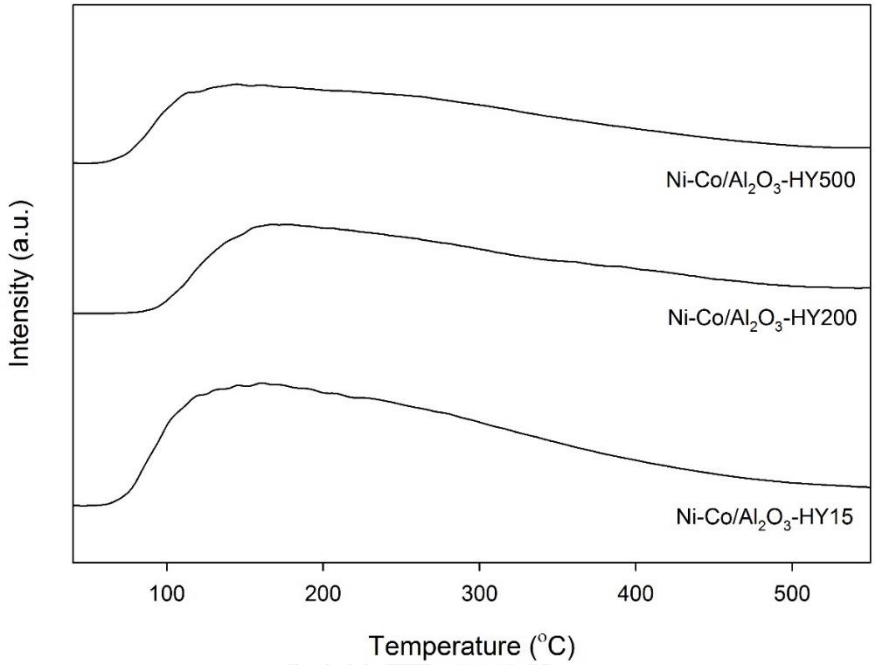

Figure 4.6 NH_3-TPD profiles of Ni-Co/Al_2O_3-HY zeolite catalysts with different Si/Al molar ratio of HY zeolites.

Table 4.2 Total acidity of Ni-Co/Al_2O_3-HY zeolite catalysts with different Si/Al molar ratio of HY zeolites.

Catalysts	Total acidity (mmol NH_3/g.cat)
Ni-Co/Al_2O_3-HY15	14.58
Ni-Co/Al_2O_3-HY200	11.21
Ni-Co/Al_2O_3-HY500	9.53

4.1.1.5 Carbon monoxide chemisorption

The metal active site, and metal dispersion of catalysts were characterized by carbon monoxide chemisorption method with reduction temperature of 500°C as shown in Table 4.3. The metal active site were ranged in 8.25-15.30 $x10^{18}$ molecules/g.cat in order: Ni-Co/Al_2O_3-HY500 > Ni-Co/Al_2O_3-HY200 > Ni-Co/Al_2O_3-HY15. The percent metal dispersion is calculated from metal active site per metal loading, so that it is proportional to the metal active site. The high metal active site led to high percent metal dispersion. The HY zeolite with Si/Al molar ratio of 500 in catalyst shown the highest active site at $15.30x10^{18}$ molecules/g.cat, resulting the highest percent metal dispersion at 1.50 %. According to the H_2-TPR results, Ni-Co/Al_2O_3-HY500 possess the high H_2 consumption and lower reduction temperature, which it may be easy reducible to metal active sites [54].

Table 4.3 CO chemisorption results of Ni-Co/Al_2O_3-HY zeolite catalysts with different Si/Al molar ratio of HY zeolites.

Catalysts	Active sites ($x10^{-18}$ molecules / g.cat)	% Dispersion
Ni-Co/Al_2O_3-HY15	8.25	0.80
Ni-Co/Al_2O_3-HY200	12.90	1.26
Ni-Co/Al_2O_3-HY500	15.30	1.50

4.1.1.6 Scanning Electron Microscopy (SEM)

The SEM images of fresh Ni-Co over Al_2O_3-HY zeolite catalysts with different Si/Al molar ratio of HY zeolites are shown in Figure 4.7. As can be seen, all catalysts have similar surface morphology. It was found that Si/Al molar ratio of HY zeolites did not affect the morphology of catalysts [47]. Figure 4.8 demonstrates the SEM images of spent Ni-Co/Al_2O_3-HY15, Ni-Co/Al_2O_3-HY200 and Ni-Co/Al_2O_3-HY500 catalysts after 180 min of reaction. All spent catalysts shown that filamentous carbon were formed and covered on surface catalysts, confirming the occurrence of methane cracking and boudouard reaction as side reaction [14].

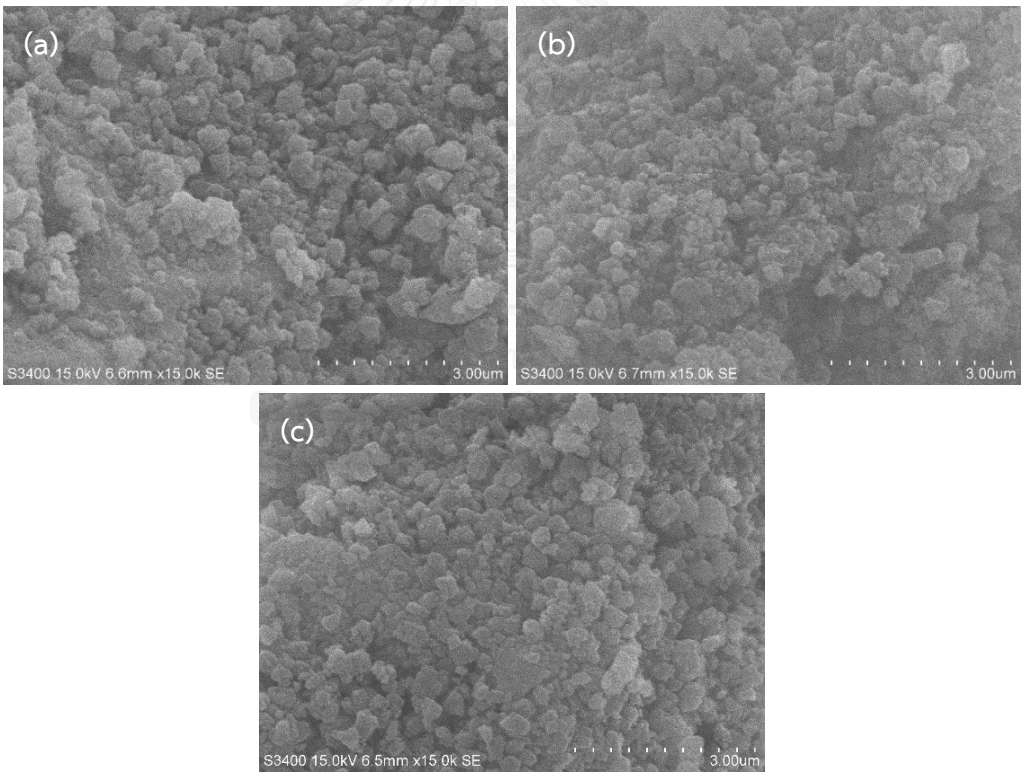

Figure 4.7 SEM images of fresh Ni-Co over Al_2O_3-HY zeolite catalysts with different Si/Al molar ratio of HY zeolites: (a) Ni-Co/Al_2O_3-HY15, (b) Ni-Co/Al_2O_3-HY200 and (c) Ni-Co/Al_2O_3-HY500.

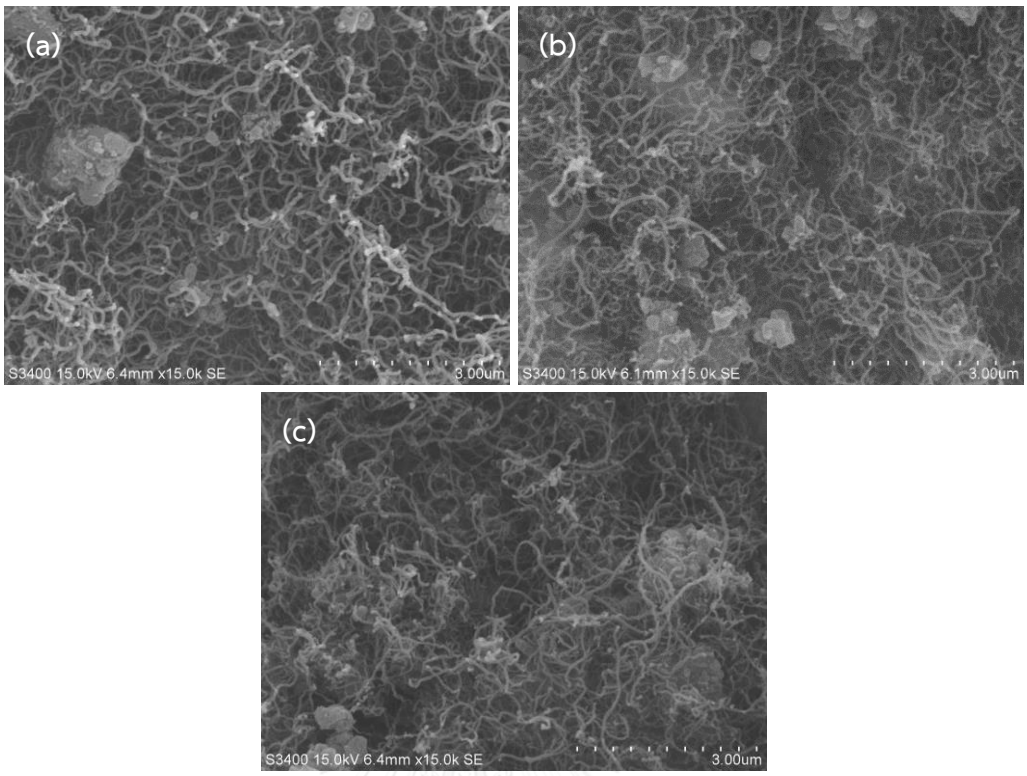

Figure 4.8 SEM images of spent catalysts with different Si/Al molar ratio of HY zeolites after 180 min of reaction: (a) Ni-Co/Al_2O_3-HY15, (b) Ni-Co/Al_2O_3-HY200 and (c) Ni-Co/Al_2O_3-HY500.

4.1.1.7 Thermo gravimetric analysis (TGA)

TGA analysis that was used for study carbon deposition of the spent catalysts are investigated in Figure 4.9. The slightly weight loss of all spent catalysts around 100 °C was occurred that was probably implied the evaporation of moisture in catalysts. As can be seen in Figure 4.9, the weight loss were observed at around 500-600 °C in the following order: Ni-Co/Al_2O_3-HY500 > Ni-Co/Al_2O_3-HY200 > Ni-Co/Al_2O_3-HY15, resulted carbon deposited over spent catalysts [55].

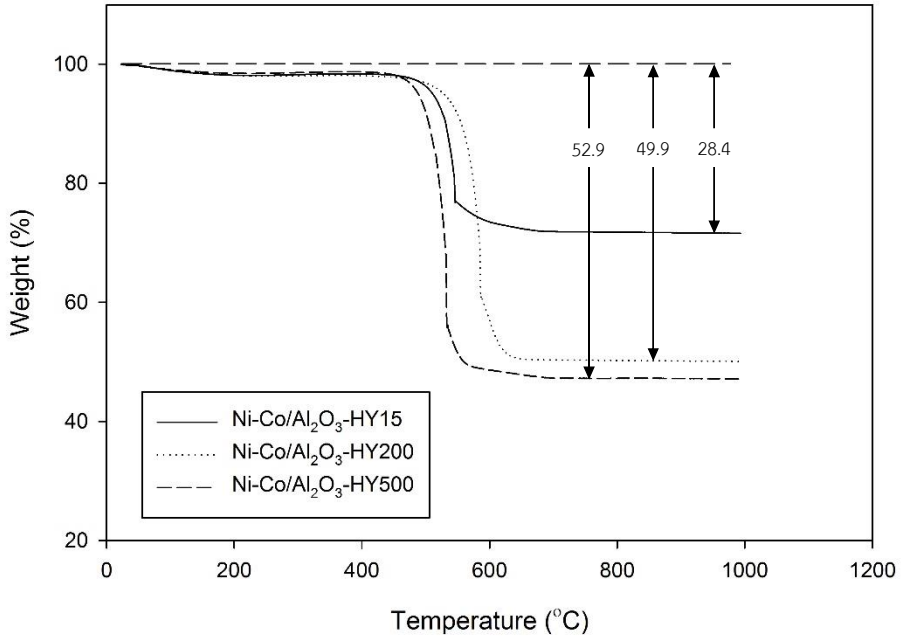

Figure 4.9 TGA results of spent catalysts with different Si/Al molar ratio of HY zeolites after 180 min of reaction.

4.1.2 Activity in carbon dioxide reforming of methane

The catalytic performances of catalysts were tested in dry reforming of methane reaction (or carbon dioxide reforming of methane) at 700 °C of reaction temperature. Before the reaction, the prepared catalysts were reduced in flowing H_2 with flow of 50 ml/min for 1 h. The conversion and product selectivity of Ni-Co/Al_2O_3-HY15, Ni-Co/Al_2O_3-HY200 and Ni-Co/Al_2O_3-HY500 at initial and final for dry reforming of methane were provided in Table 4.4. The CO_2 conversion is higher than the CH_4 conversion in each catalysts that this is due to the occurrence of reverse water-gas shift reaction (RWGS: $CO_2 + H_2 \longrightarrow H_2O + CO$) [56]. Figure 4.10 and Figure 4.11 illustrate the CH_4 and CO_2 conversion of catalysts during 180 min of time on stream. Ni-Co over Al_2O_3-HY zeolites with different Si/Al molar ratios of HY zeolite (HY15, HY200 and HY500) provided the CO_2 and CH_4 conversions in the range 48.5-77.7% and 54.8-81.8%,

respectively, in order: Ni-Co/Al_2O_3-HY500 > Ni-Co/Al_2O_3-HY200 > Ni-Co/Al_2O_3-HY15. The H_2 and CO selectivity of catalysts during 180 min of time on stream are shown in Figure 4.12 and Figure 4.13, respectively. The selectivity was calculated based on amount of H_2 and CO product. The results show that the H_2 selectivity is lower than the CO selectivity, confirming the occurrence of RWGS reaction [57]. Ni-Co/Al_2O_3-HY500 exhibited higher the H_2 selectivity than the others in contrast to the CO selectivity. According to CO chemisorption results, Ni-Co/Al_2O_3-HY500 possess the highest amount of metal active site, corresponding to the highest metal dispersion. So, it had high Ni and CO active metal over support, where the reactant gases can be accessible [54, 58]. H_2-TPR results indicated that HY500 in catalysts shown higher intensity of reduction peaks than the others, indicating easier reducibility. The acidity of catalysts from NH_3-TPD decreased with increasing Si/Al molar ratios of HY zeolites. Ni-Co/Al_2O_3-HY15 exhibited higher total acidity that may hamper CO_2 adsorption and activation resulting led to lower catalytic activity [59, 60].

Table 4.4 The conversion and product selectivity of Ni-Co/Al_2O_3-HY15, Ni-Co/Al_2O_3-HY200 and Ni-Co/Al_2O_3-HY500.

Catalysts	Conversion (%)				Product selectivity (%)			
	Initial[a]		Final[b]		Initial[a]		Final[b]	
	CH_4	CO_2	CH_4	CO_2	H_2	CO	H_2	CO
Ni-Co/Al_2O_3-HY15	49.6	53.9	48.5	54.8	36.6	63.4	35.0	65.0
Ni-Co/Al_2O_3-HY200	72.6	80.1	74.1	80.6	40.5	59.5	41.3	58.7
Ni-Co/Al_2O_3-HY500	74.5	79.9	77.7	81.8	41.9	58.1	42.8	57.2

[a] After 30 min of reaction

[b] After 180 min of reaction

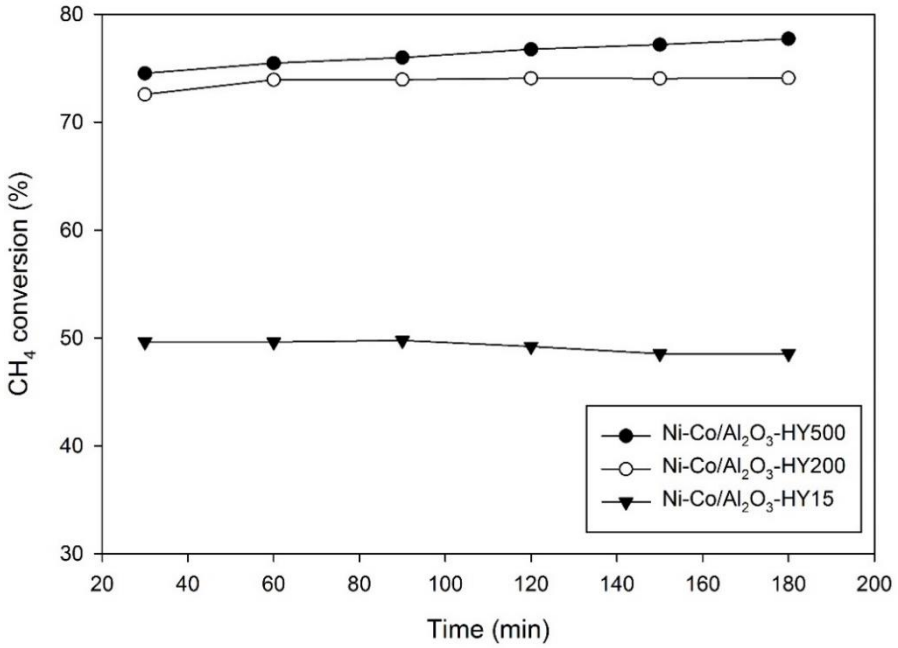

Figure 4.10 CH_4 conversion of Ni-Co over Al_2O_3-HY zeolites with different Si/Al molar ratios of HY zeolite at 700 °C.

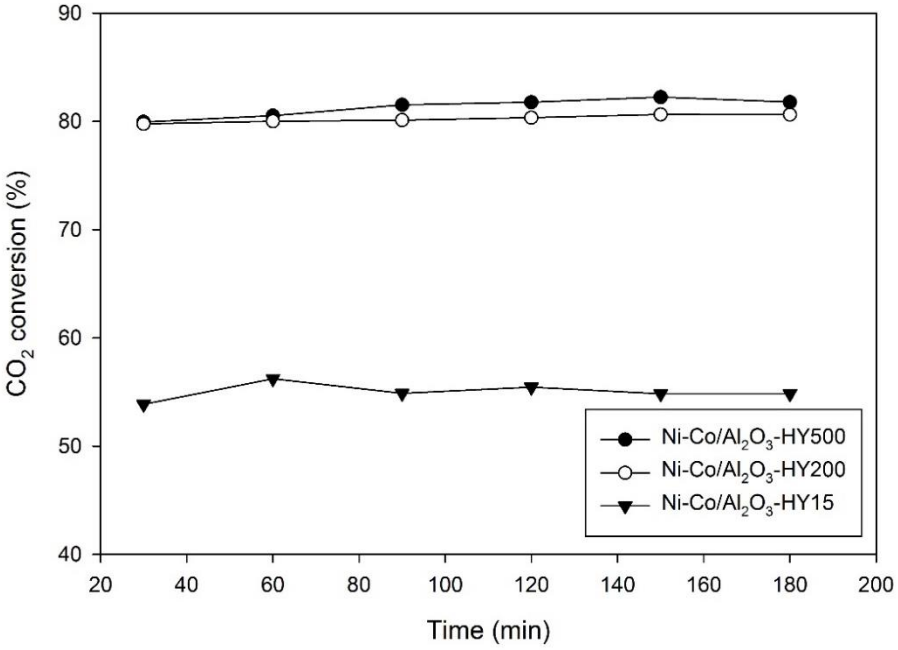

Figure 4.11 CO_2 conversion of Ni-Co over Al_2O_3-HY zeolites with different Si/Al molar ratios of HY zeolite at 700 °C.

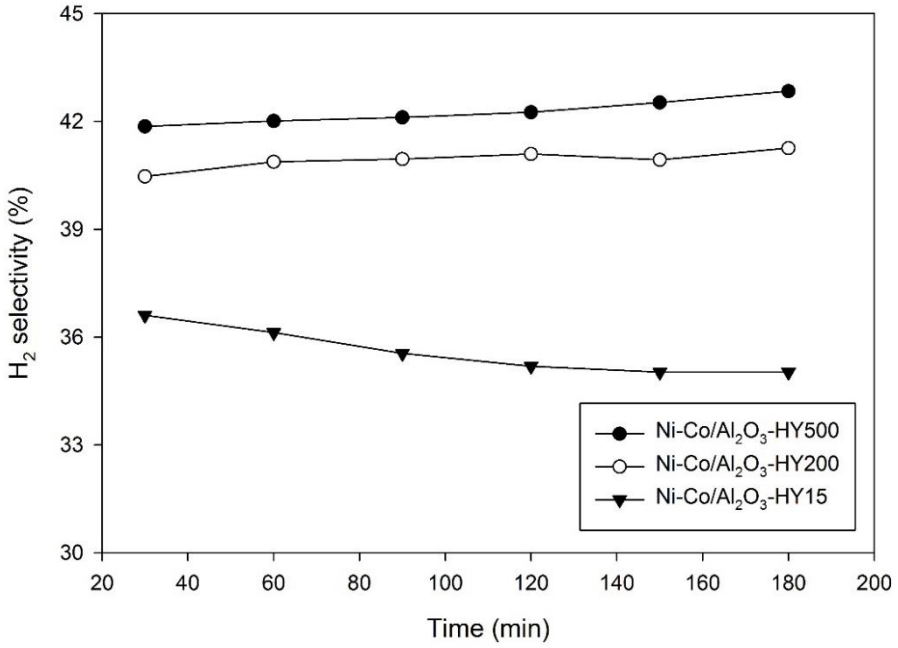

Figure 4.12 H_2 selectivity of Ni-Co over Al_2O_3-HY zeolites with different Si/Al molar ratios of HY zeolite at 700 °C.

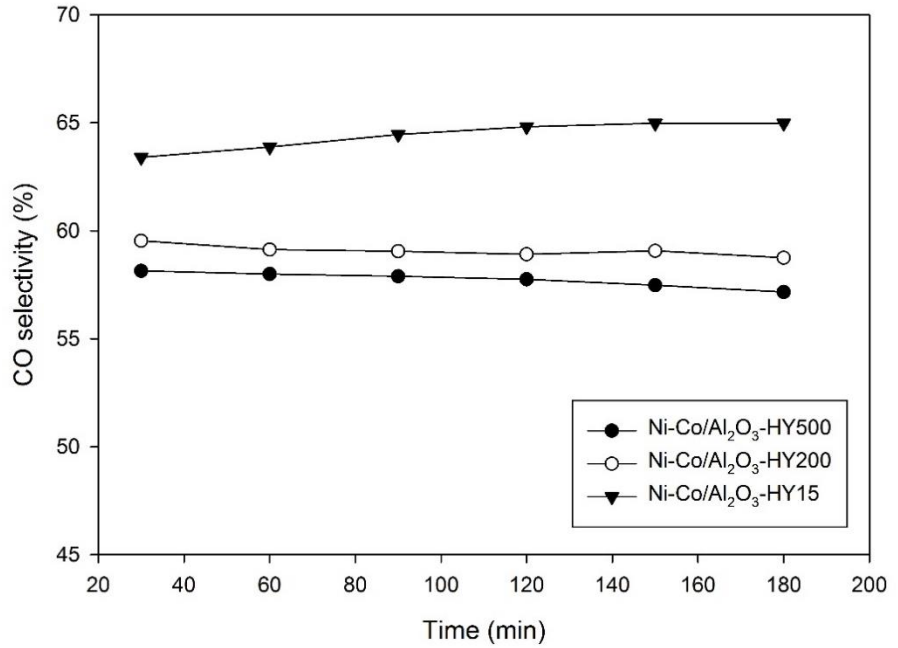

Figure 4.13 CO selectivity of Ni-Co over Al_2O_3-HY zeolites with different Si/Al molar ratios of HY zeolite at 700 °C.

4.2 The effect of support ratio of Al_2O_3 and selected HY zeolite from the first part and compare to the Al_2O_3 support and HY zeolite support in bimetallic catalysts.

The catalyst nomenclatures are represent as below:

Ni-Co/Al_2O_3 represents the catalyst which have Ni and Co over Al_2O_3 support.

Ni-Co/3Al_2O_3-1HY500 represents the catalyst which have Ni and Co over Al_2O_3-HY500 support in Al_2O_3 and HY500 support ratio of 3:1.

Ni-Co/1Al_2O_3-1HY500 represents the catalyst which have Ni and Co over Al_2O_3-HY zeolite support in Al_2O_3 and HY500 support ratio of 1:1.

Ni-Co/1Al_2O_3-3HY500 represents the catalyst which have Ni and Co over Al_2O_3-HY zeolite support in Al_2O_3 and HY500 support ratio of 1:3.

Ni-Co/HY500 represents the catalyst which have Ni and Co over HY zeolite support with Si/Al molar ratio of 500.

4.2.1 Catalyst characterization

4.2.1.1 X-Ray diffraction pattern (XRD)

The X-ray diffraction (XRD) patterns of Al_2O_3, HY zeolite, and Al_2O_3-HY zeolite supports with different Al_2O_3 and HY500 support ratio (3:1, 1:1 and 1:3) are shown in Figure 4.14. It was observed that XRD pattern of Al_2O_3 support shown two peaks at 2θ = 45.6° and 66.7° which are ascribed to alumina crystalline phases. HY zeolite were observed at 2θ = 20.3°, 23.7°, 27.0°, 31.8°, 34.2°, 38.4° and 54.6° which are typical of zeolite faujasite [37]. The mixed Al_2O_3 and HY zeolite in all ratios had similar pattern to alumina and zeolite faujasite. In comparison of XRD patterns in each supports, the

intensity of HY500 increased with increasing of HY500 content in the mixed Al_2O_3-HY500, whereas the intensity of Al_2O_3 decreased [41].

The XRD patterns of the bimetallic Ni-Co over Al_2O_3, HY500 and Al_2O_3-HY500 catalysts with support ratios of 3:1, 1:1, and 1:3 are illustrated in Figure 4.15. For all XRD patterns, crystalline phase assigned to nickel oxide and/or nickel aluminate was observed with diffraction peaks at 2θ = 43.5° and 64.5° whereas crystalline phase assigned to cobalt oxide and/or cobalt aluminate was observed with diffraction peaks at 36.9°, 43.5°, 59.4° and 64.5° [43]. Diffraction peak of Al_2O_3-HY zeolite support in bimetallic catalysts did not change indicating no phase transformation during incipient wetness impregnation [44].

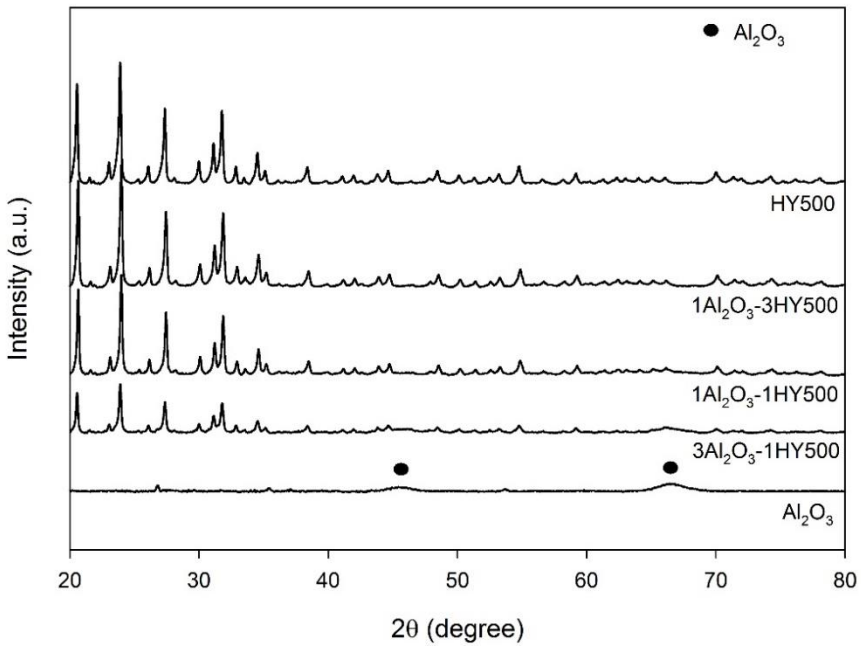

Figure 4.14 XRD patterns of Al_2O_3, HY zeolite, and Al_2O_3-HY zeolite supports with different Al_2O_3 and HY500 support ratio (3:1, 1:1 and 1:3).

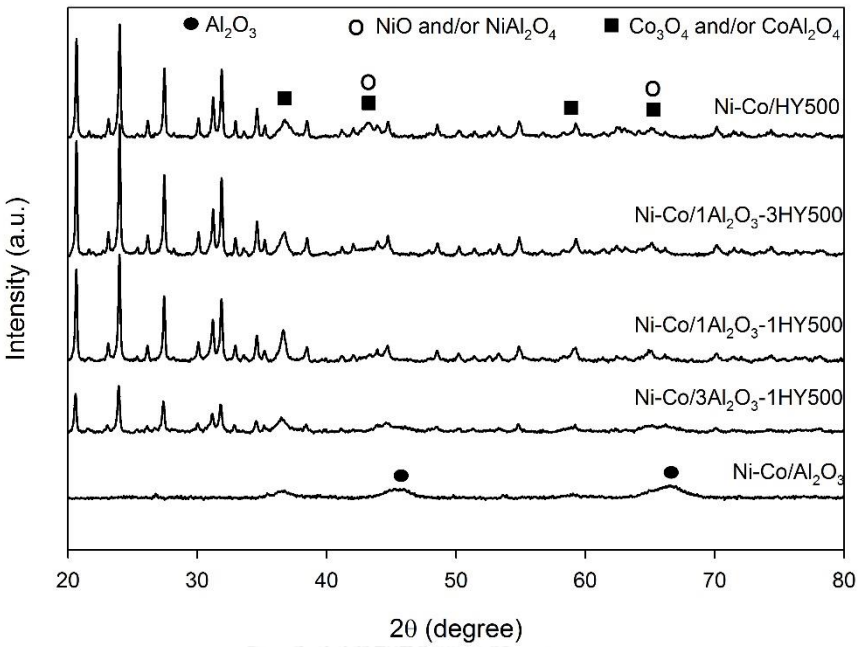

Figure 4.15 XRD patterns of the Ni-Co over Al_2O_3, HY500 and Al_2O_3-HY500 catalysts with support ratios of 3:1, 1:1, and 1:3.

4.2.1.2 Nitrogen adsorption-desorption

The BET surface area, pore volume and pore size of support and catalysts were determined by nitrogen adsorption-desorption technique using Brunauer–Emmett–Teller (BET) method and Barret-Joyner-Halenda (BJH) method, and there are given in Table 4.5. Al_2O_3 and HY500 support had BET surface area of 200 and 793 m^2/g, respectively, whereas mixed 3Al_2O_3-1HY500, 1Al_2O_3-1HY500 and 1Al_2O_3-3HY500 support had BET surface area of 502, 645 and 742 m^2/g, respectively. The BET surface area of support increased with an increase HY500 content in mixed Al_2O_3-HY500, resulted the high BET area of HY500 [61]. Loading Ni-Co catalysts possess the BET surface area in range of 156-687 m^2/g, which are lower than each their support. This is implied that some pore may be blocked by Ni and Co species, meaning the formation of Ni and Co metal in the pore of support [62]. The pore volume of support and

catalysts were ranged between 0.29-0.31 cm^3/g and 0.23-0.27 cm^3/g, respectively, illustrating metals probably block the pore [45].

Table 4.5 The physiochemical properties of supports and Ni-Co over Al_2O_3, HY500 and Al_2O_3-HY500 catalysts with support ratios of 3:1, 1:1, and 1:3.

Catalysts	BET surface area (m^2/g)	Pore volume (cm^3/g)	Pore size (nm)
Al_2O_3	200	0.29	3.8
$3Al_2O_3$-1HY500	502	0.31	5.2
$1Al_2O_3$-1HY500	645	0.29	6.7
$1Al_2O_3$-3HY500	742	0.29	7.0
HY500	793	0.29	7.9
Ni-Co/Al_2O_3	156	0.23	3.9
Ni-Co/$3Al_2O_3$-1HY500	414	0.24	5.2
Ni-Co/$1Al_2O_3$-1HY500	542	0.27	7.0
Ni-Co/$1Al_2O_3$-3HY500	639	0.24	7.0
Ni-Co/HY500	687	0.24	7.5

The N_2 adsorption-desorption isotherm of Al_2O_3, HY500 and Al_2O_3-HY zeolites support, and Ni-Co/Al_2O_3-HY500 catalysts with different ratios of Al_2O_3 and HY500 are provided in Figure 4.16 and Figure 4.17, respectively. The isotherms of Al_2O_3 and Ni-Co/Al_2O_3 can be classified as a type IV isotherm with H2-shaped hysteresis loops, corresponding to mesoporous structure [46]. While the others support and catalysts exhibited a type IV isotherm with H3-shaped hysteresis loops that are implied micro-mesoporous structure [41].

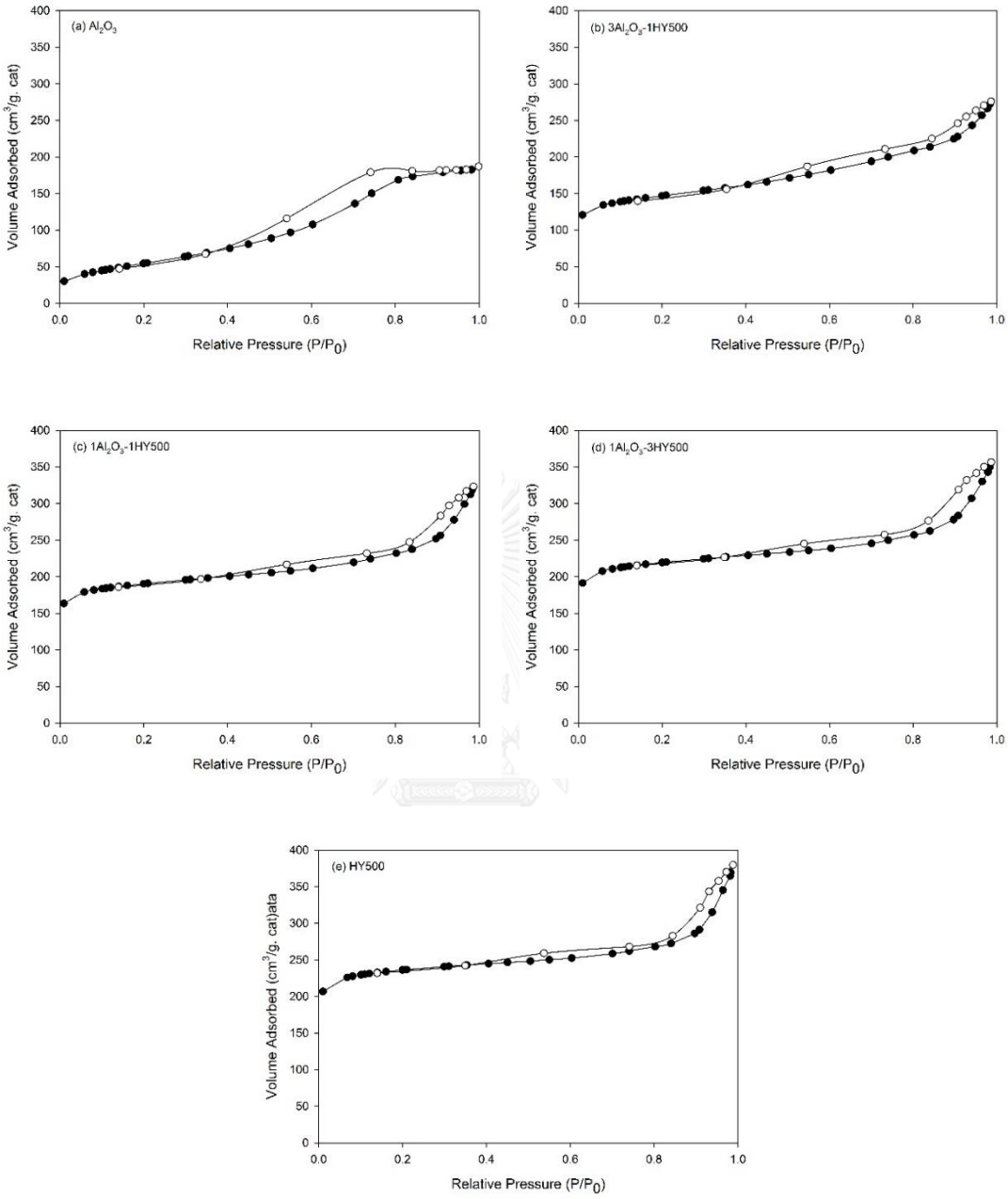

Figure 4.16 N_2 adsorption-desorption isotherm for Al_2O_3, HY500 and Al_2O_3-HY zeolite support.

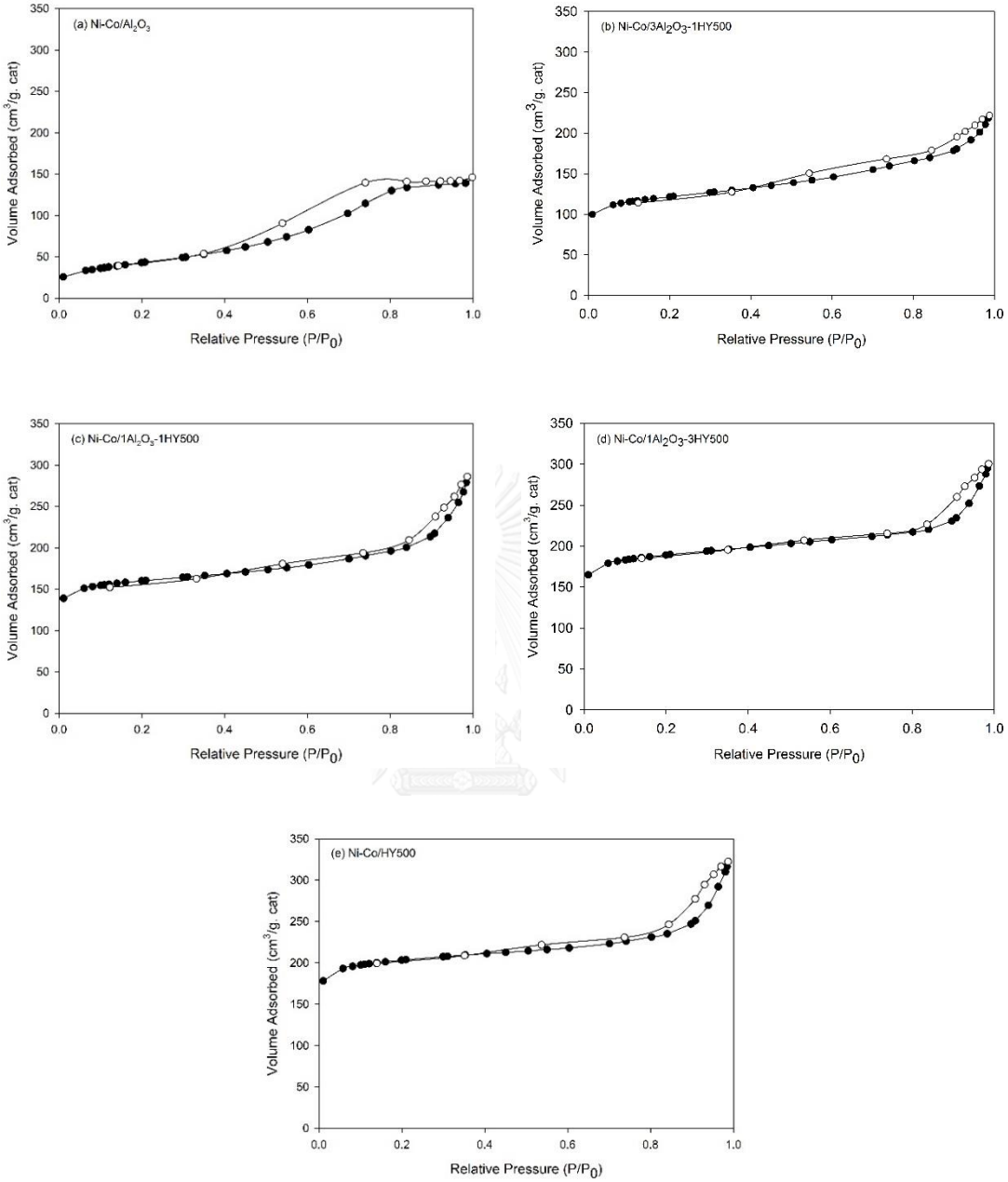

Figure 4.17 N_2 adsorption-desorption isotherm of Ni-Co over Al_2O_3, HY500 and Al_2O_3-HY zeolite catalyst.

4.2.1.3 Hydrogen temperature programmed reduction (H_2-TPR)

Hydrogen temperature programmed reduction (H_2-TPR) was used for investigating the reduction behavior of the samples. The H_2-TPR profiles of bimetallic Ni-Co over Al_2O_3, HY500 and Al_2O_3-HY500 with different support ratios of 3:1, 1:1 and 1:3 are displayed in Figure 4.18. Ni-Co/Al_2O_3 and Ni-Co/3Al_2O_3-1HY500 exhibited two peaks, suggesting the reduction of Ni and Co oxide with weak interaction with supports [35]. In addition to those catalysts, Ni-Co/1Al_2O_3-1HY500 and Ni-Co/1Al_2O_3-3HY500 showed the third peak implying the reduction of Ni and Co species with strong interaction with support [54]. However, Ni-Co/HY500 exhibited two peaks that was implied the reduction of weak and strong metal-supports interaction. As can be seen in Figure 4.18, the reduction temperature shifted to lower temperature with increasing the content of HY500 in support, which could be ascribed to a decrease the metal-supports interaction and suggested that it was easy to reducibility of metal.

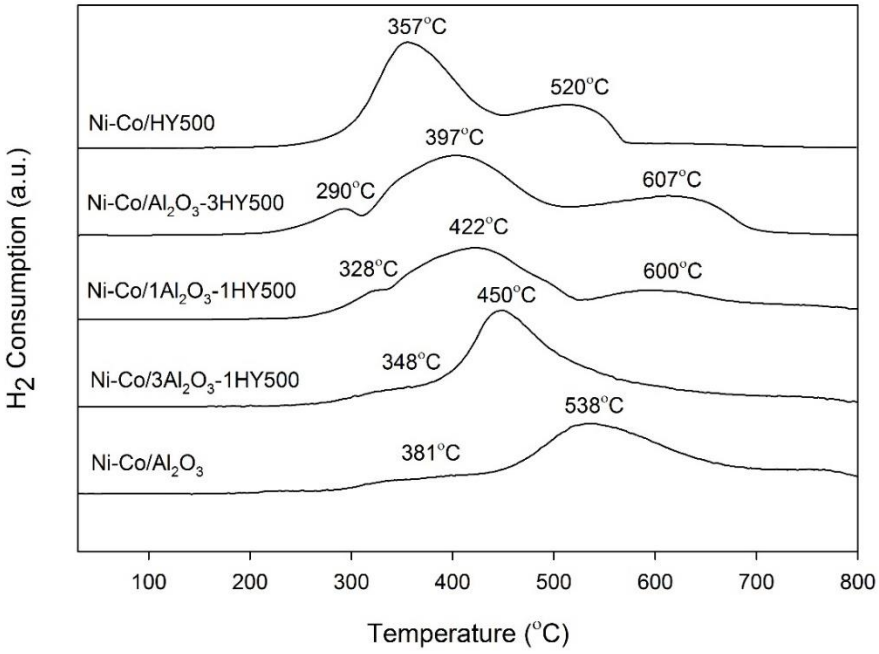

Figure 4.18 H_2-TPR profiles of bimetallic Ni-Co over Al_2O_3, HY500 and Al_2O_3-HY500.

4.2.1.4 Ammonia temperature program desorption (NH_3-TPD)

Ammonia temperature program desorption (NH_3-TPD) was used for evaluating the acidity on surface of the loading Ni-Co catalysts with different ratios of Al_2O_3 and HY500 supports. The amount of desorbed ammonia corresponds to the total surface acidity of the catalysts. In addition, the desorption temperature of desorbed ammonia corresponds to the acid strength on surface of the catalysts.

NH_3-TPD profiles of the loading Ni-Co catalysts with different ratios of Al_2O_3-HY500 supports are shown in Figure 4.19. Ni-Co/Al_2O_3 and Ni-Co/3Al_2O_3-1HY500 exhibited only one desorption peak at low temperature indicating the presence of weak acid sites, whereas Ni-Co/1Al_2O_3-1HY500, Ni-Co/1Al_2O_3-3HY500 and Ni-Co/HY500 exhibited two desorption peaks at low temperature and high temperature, meaning two type of the acid sites. The latter peak is attributed to the strong acid sites, which are responsible for the growth of carbonaceous deposited on catalysts [63]. The total acidity of Ni-Co over Al_2O_3, HY500 and Al_2O_3-HY500 catalysts with ratios of 3:1, 1:1 and 1:3 are summarized in Table 4.6. The total acidity of catalysts decreased in the following order: Ni-Co/Al_2O_3 > Ni-Co/3Al_2O_3-1HY500 > Ni-Co/1Al_2O_3-1HY500 > Ni-Co/1Al_2O_3-3HY500 > Ni-Co/HY500. The results showed that total acidity decreased with an increasing HY500 content in mixed supports. It is known that the high acidity may hamper CO_2 adsorption and activation resulting led to lower catalytic activity [53, 58].

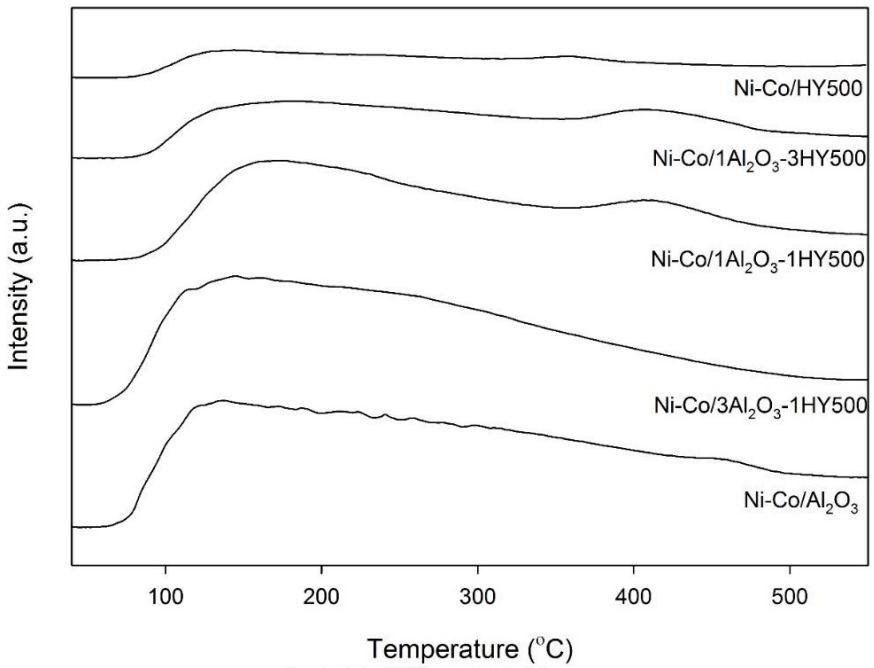

Figure 4.19 NH_3-TPD profiles of Ni-Co over Al_2O_3, HY500 and Al_2O_3-HY500 catalysts with ratios of 3:1, 1:1 and 1:3.

Table 4.6 The total acidity of Ni-Co over Al_2O_3, HY500 and Al_2O_3-HY500 catalysts with ratios of 3:1, 1:1 and 1:3.

Catalysts	Total acidity (mmol NH_3/g.cat)
Ni-Co/Al_2O_3	12.05
Ni-Co/3Al_2O_3-1HY500	9.53
Ni-Co/1Al_2O_3-1HY500	7.05
Ni-Co/1Al_2O_3-3HY500	5.26
Ni-Co/HY500	3.00

4.2.1.5 Carbon monoxide chemisorption

The metal active site, and metal dispersion of catalyst were characterized by carbon monoxide chemisorption method with reduction temperature of 500°C as shown in Table 4.7. It was found that different support ratio of Al_2O_3 and HY zeolite in Ni-Co over alumina-HY zeolite affected metal active site and metal dispersion. The metal active site were ranged in 0.07-20.37 $x10^{18}$ molecules/g.cat in order: Ni-Co/1Al_2O_3-3HY500 > Ni-Co/1Al_2O_3-1HY500 > Ni-Co/3Al_2O_3-1HY500 > Ni-Co/HY500 > Ni-Co/Al_2O_3. The percent metal dispersion is calculated from metal active site per metal loading, so that it is proportional to the metal active site. The high metal active site led to high percent metal dispersion [64]. The support ratio of Al_2O_3 and HY zeolite of 1:3 in catalyst shown the highest active site at 20.73 $x10^{18}$ molecules/g.cat, resulting the highest percent metal dispersion at 2.02 %. According to the H_2-TPR results, Ni-Co/Al_2O_3-HY500 possess the high H_2 consumption and lower reduction temperature than other, which it may be easy to reduce to metal active sites.

Table 4.7 CO chemisorption results of Ni-Co over Al_2O_3, HY500 and Al_2O_3-HY500 catalysts with different support ratios.

Catalysts	Active sites ($x10^{-18}$ molecules / g.cat)	% Dispersion
Ni-Co/Al_2O_3	0.07	0.03
Ni-Co/3Al_2O_3-1HY500	15.39	1.50
Ni-Co/1Al_2O_3-1HY500	17.47	1.70
Ni-Co/1Al_2O_3-3HY500	20.73	2.02
Ni-Co/HY500	14.72	1.43

4.2.1.6 Scanning Electron Microscopy (SEM)

The morphology of fresh Ni-Co over Al_2O_3, HY500 and Al_2O_3-HY500 catalysts with $3Al_2O_3$-1HY500, $1Al_2O_3$-1HY500 and $1Al_2O_3$-3HY500 studied by Scanning Electron Microscopy (SEM) are shown in Figure 4.20. Most catalysts have similar surface morphology except Ni-Co/Al_2O_3 [65]. Figure 4.21 demonstrates the SEM images of spent Ni-Co/Al_2O_3, Ni-Co/$3Al_2O_3$-1HY500, Ni-Co/$1Al_2O_3$-1HY500 Ni-Co/$1Al_2O_3$-3HY500 and Ni-Co/HY500 catalysts after 180 min of reaction. All spent catalysts showed that filamentous carbon were formed and covered on surface catalysts [3].

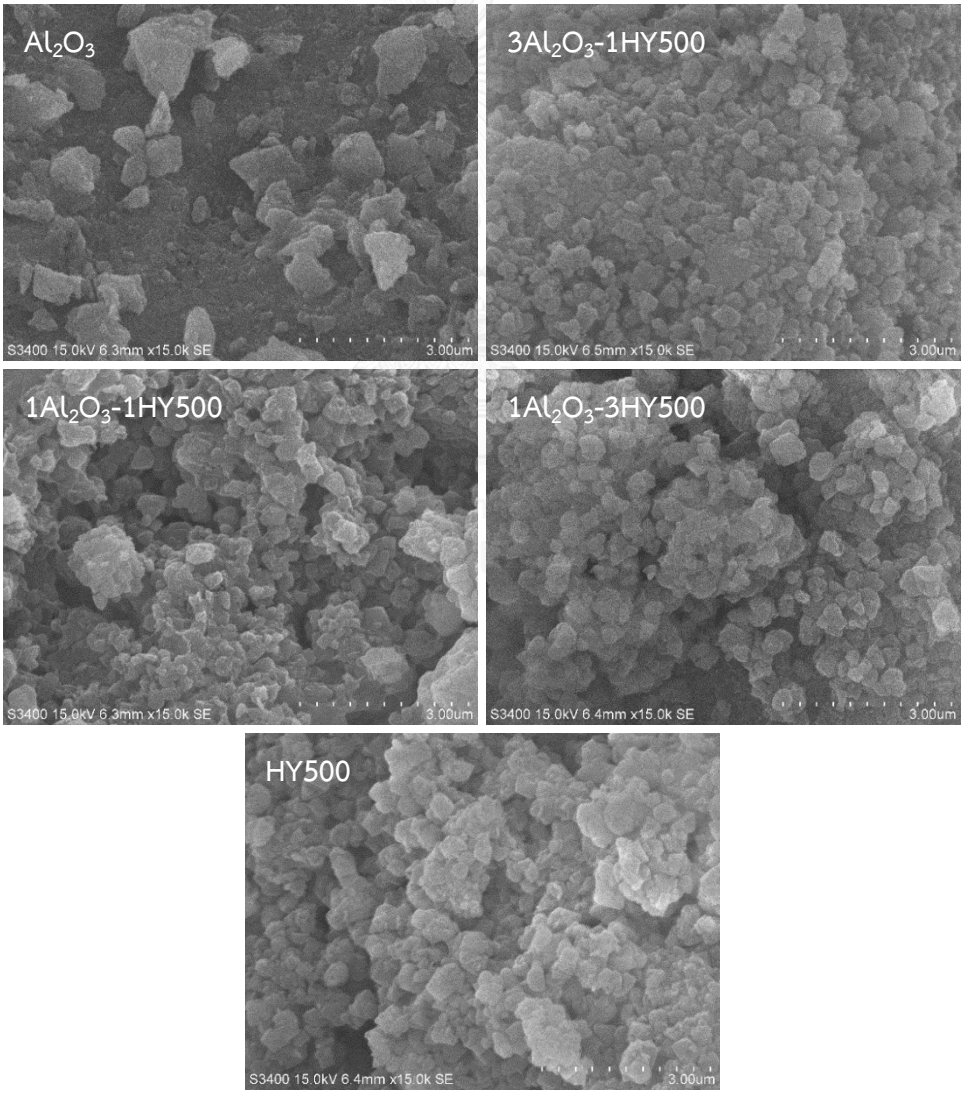

Figure 4.20 SEM images of fresh catalysts with different support ratio.

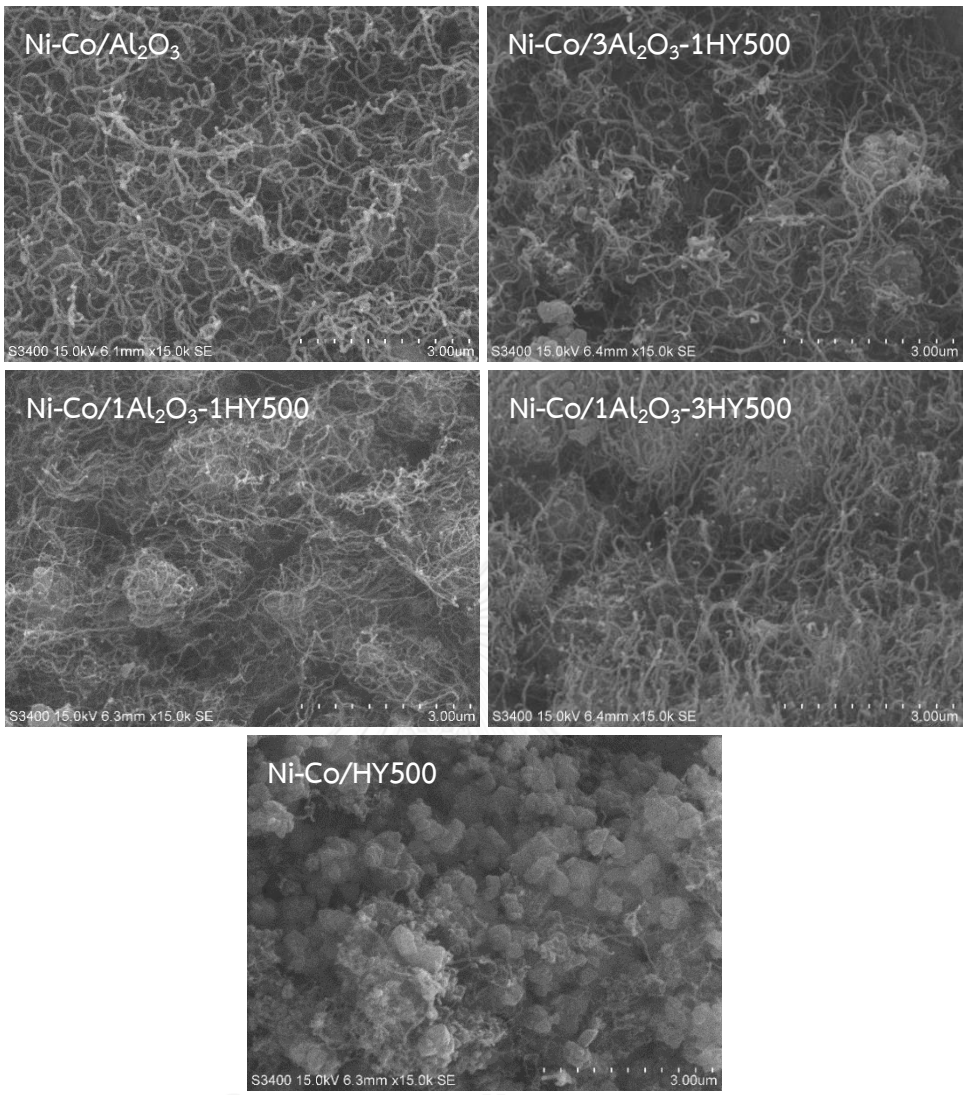

Figure 4.21 SEM images of spent Ni-Co/Al_2O_3, Ni-Co/3Al_2O_3-1HY500, Ni-Co/1Al_2O_3-1HY500, Ni-Co/1Al_2O_3-3HY500 and Ni-Co/HY500 catalysts after 180 min of reaction.

4.2.1.7 Thermo gravimetric analysis (TGA)

TGA analysis that was used for study carbon deposition of the spent catalysts are investigated in Figure 4.22. The slightly weight loss of all spent catalysts around 100 °C was occurred that was probably implied the evaporation of moisture in catalysts. As can be seen in Figure 4.22, the weight loss were observed at around 500-600 °C which Ni-Co/1Al_2O_3-3HY500 possessed the highest weight loss resulted much carbon deposited over spent catalysts [55].

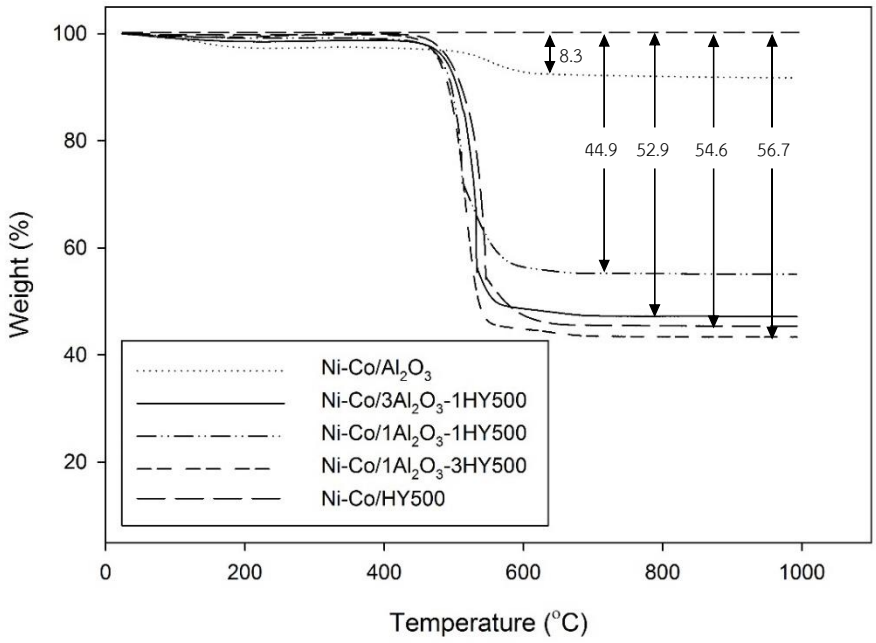

Figure 4.22 TGA results of spent catalysts with different support ratio after 180 min of reaction.

4.2.2 Activity in carbon dioxide reforming of methane

The catalytic performances of catalysts were tested in carbon dioxide reforming with methane at 700 °C of reaction temperature. Before the reaction, the prepared catalysts were reduced in flowing H_2 with flow of 50 ml/min for 1 h. The conversion and product selectivity of Ni-Co/Al_2O_3, Ni-Co/3Al_2O_3-1HY500, Ni-Co/1Al_2O_3-1HY500, Ni-Co/1Al_2O_3-3HY500 and Ni-Co/HY500 at initial and final for dry reforming of methane were provided in Table 4.8. The CO_2 conversion is higher than the CH_4 conversion in each catalysts that this is due to the occurrence of reverse water-gas shift reaction (RWGS: $CO_2 + H_2 \longrightarrow H_2O + CO$) [20]. Figure 4.23 and Figure 4.24 illustrate the CH_4 and CO_2 conversion of catalysts during 180 min of time on stream. Ni-Co over Al_2O_3, HY500 and Al_2O_3-HY500 with different ratios of Al_2O_3 and HY500 (1:3, 1:1 and 1:3) provided the CH_4 and CO_2conversions in the range 71.1-82.6% and 74.0-84.3%, respectively, in order: Ni-Co/1Al_2O_3-3HY500 > Ni-Co/3Al_2O_3-1HY500 > Ni-Co/1Al_2O_3-1HY500 > Ni-Co/HY500 > Ni-Co/Al_2O_3. The H_2 and CO selectivity of catalysts during 180 min of time on stream are shown in Figure 4.25 and Figure 4.26, respectively. The selectivity was calculated based on amount of H_2 and CO product. The results show that the H_2 selectivity is lower than the CO selectivity, confirming the occurrence of RWGS reaction [66]. Ni-Co/1Al_2O_3-3HY500 exhibited higher the H_2 selectivity than the other catalysts in contrast to the CO selectivity. From H_2-TPR results, it indicated that support ratio of 1:3 in catalysts shown low reduction temperature, indicating easier reducibility. According to CO chemisorption, Ni-Co/1Al_2O_3-3HY500 possess the highest amount of Ni and Co active site, corresponding to the highest metal dispersion. So, it had high Ni and CO active metal on catalyst, where the reactant gases can be accessible. The acidity of catalysts from NH_3-TPD decreased with an increasing HY500 content in support. Also, the higher acidity may hamper CO_2 adsorption and activation resulting in lower catalytic activity [53].

In comparing catalysts with pure supports and mixed Al_2O_3-HY500 supports, it was found that the mixed supports possess higher amount of active sites and metal dispersion than pure supports, resulting higher both reactant conversion and product selectivity. Thus, the mixed supports had synergy between Al_2O_3 and HY500 which promoted each other leading to higher catalytic performance.

Table 4.8 The conversion and product selectivity of Ni-Co/Al_2O_3, Ni-Co/3Al_2O_3-1HY500, Ni-Co/1Al_2O_3-1HY500, Ni-Co/1Al_2O_3-3HY500 and Ni-Co/HY500 for carbon dioxide reforming with methane.

Catalysts	Conversion (%)				Product selectivity (%)			
	Initial[a]		Final[b]		Initial[a]		Final[b]	
	CH_4	CO_2	CH_4	CO_2	H_2	CO	H_2	CO
Ni-Co/Al_2O_3	69.6	74.6	71.1	74.0	38.7	61.3	40.0	60.0
Ni-Co/3Al_2O_3-1HY500	74.5	79.9	77.7	81.8	41.9	58.1	42.8	57.2
Ni-Co/1Al_2O_3-1HY500	78.3	79.0	79.9	79.8	41.4	58.6	42.6	57.4
Ni-Co/1Al_2O_3-3HY500	82.6	86.3	82.6	84.3	45.6	54.4	46.0	54.0
Ni-Co/HY500	75.2	78.5	73.2	75.7	41.1	58.9	40.9	59.1

[a] After 30 min of reaction

[b] After 180 min of reaction

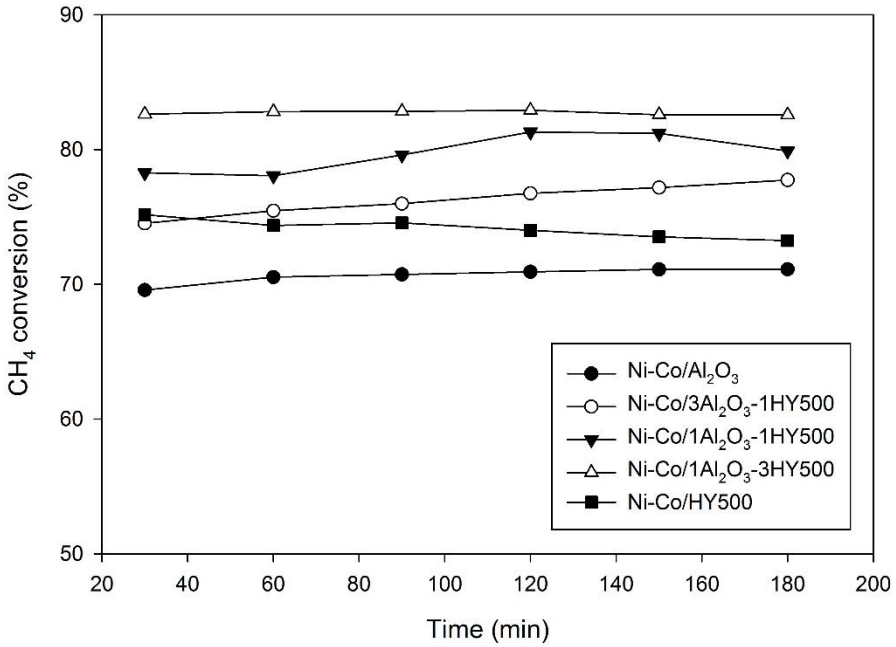

Figure 4.23 CH_4 conversion of Ni-Co over Al_2O_3, HY500 and Al_2O_3-HY zeolites with different ratios at 700 °C.

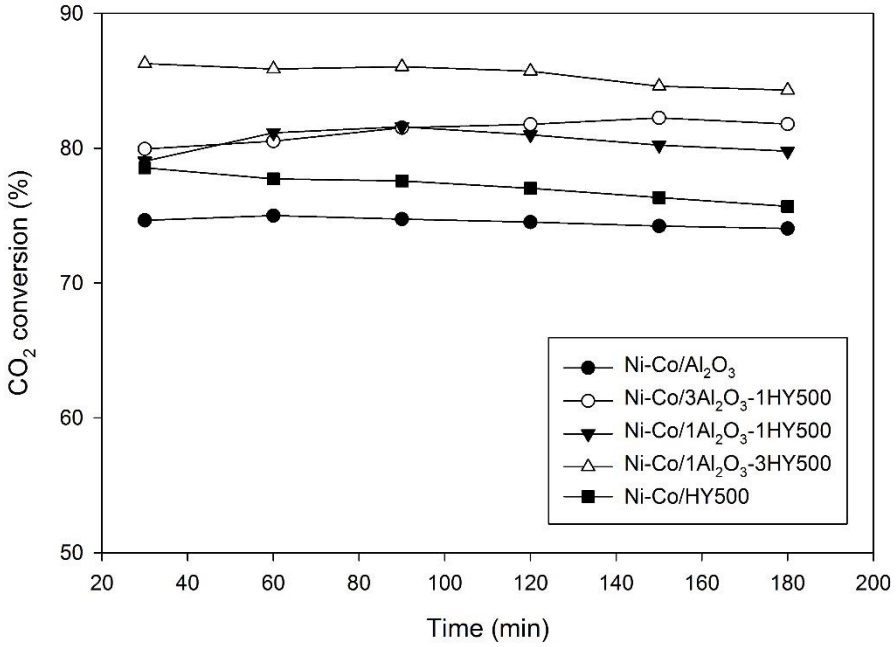

Figure 4.24 CO_2 conversion of Ni-Co over Al_2O_3, HY500 and Al_2O_3-HY zeolites with different ratios at 700 °C.

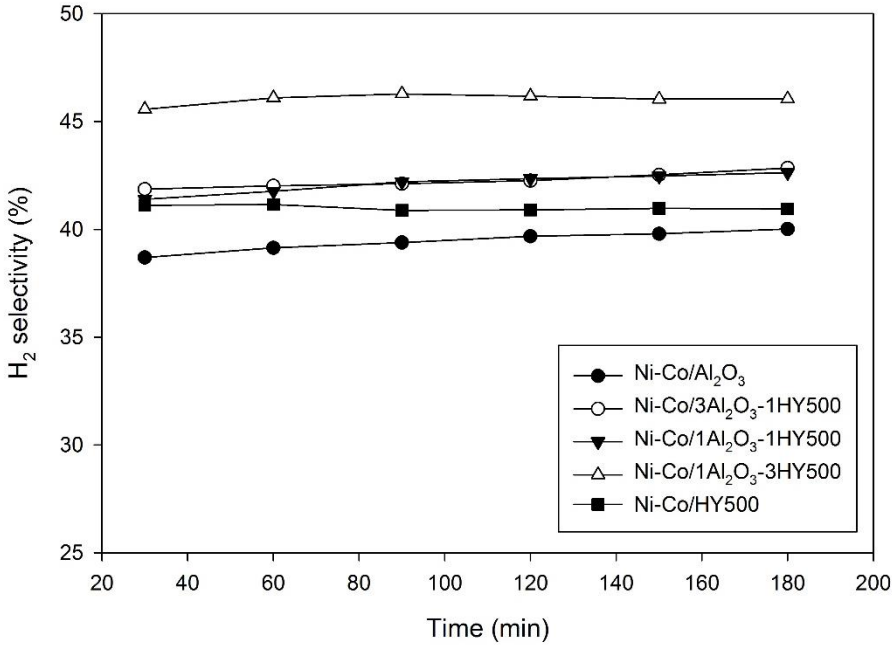

Figure 4.25 H_2 selectivity of Ni-Co over Al_2O_3, HY500 and Al_2O_3-HY zeolites with different ratios at 700 °C.

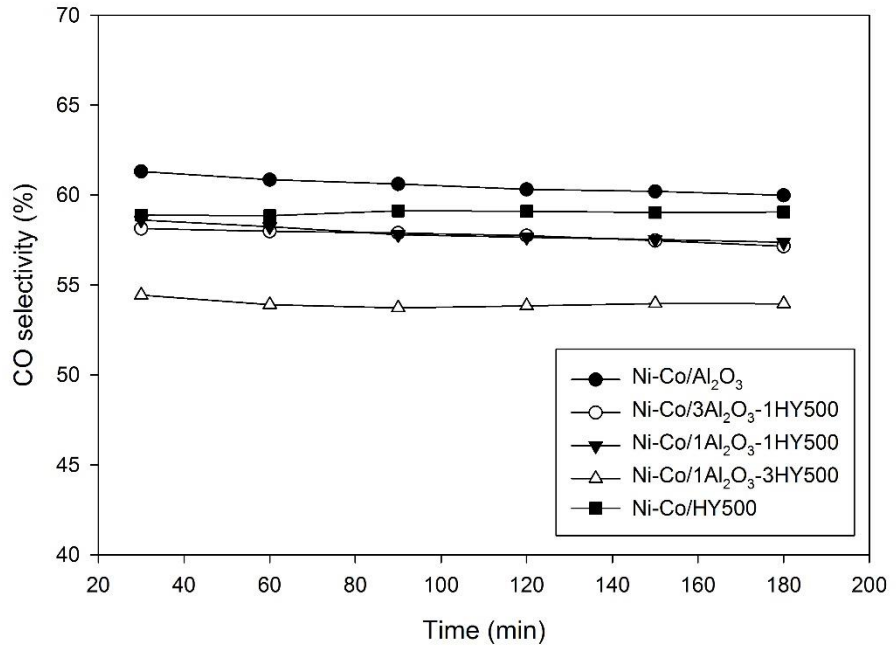

Figure 4.26 CO selectivity of Ni-Co over Al_2O_3, HY500 and Al_2O_3-HY zeolites with different ratios at 700 °C.

From two parts, all catalysts were calculated on H_2 and CO yield, and H_2/CO ratio as summarized in Table 4.9. It is indicated that Ni-Co over Al_2O_3-HY500 with support ratio of 1:3 exhibited highest H_2 yield at 37.8% and highest H_2/CO ratio which was closer to 1 than the other catalysts. Thus, Ni-Co/1Al_2O_3-3HY500 was the best catalyst for carbon dioxide reforming of methane in this research. The commercial Ni/Al_2O_3 catalyst gave CH_4 conversion at 78% that was lower than catalysts in this research [67]. From previous research, S. Thongratkeaw (2015) [68] studied monometallic and bimetallic Ni-Co over Al_2O_3-ZSM-5 catalysts. It was found that 5wt.%Ni and 5wt.%Co over Al_2O_3-ZSM-5 in support ratio of 3:1 showed the highest H_2 yield of 34.0%. In comparison, Ni-Co over Al_2O_3-HY500 with support ratio of 1:3 exhibited better catalytic performance than Ni-Co over Al_2O_3-ZSM-5 in support ratio of 3:1 and commercial catalyst. Hence, the best catalysts in this research can improve the catalytic performance in carbon dioxide reforming of methane.

Table 4.9 Yield and H_2/CO ratio of bimetallic catalysts for CO_2 reforming of CH_4.

Catalysts	Yield (%)		H_2/CO
	H_2	CO	
Ni-Co/Al_2O_3-HY15	18.3	36.0	0.54
Ni-Co/Al_2O_3-HY200	33.3	49.2	0.70
Ni-Co/Al_2O_3-HY500	34.9	48.2	0.74
Ni-Co/Al_2O_3	29.2	46.0	0.67
Ni-Co/3Al_2O_3-1HY500	34.9	48.2	0.74
Ni-Co/1Al_2O_3-1HY500	35.8	50.6	0.75
Ni-Co/1Al_2O_3-3HY500	37.8	47.1	0.85
Ni-Co/HY500	31.1	46.9	0.69

CHAPTER V
CONCLUSIONS AND RECOMMENDATION

5.1 Conclusions

In this study, the effect of different Si/Al molar ratio of HY zeolite (15, 200 and 500) in Ni-Co over Al_2O_3-HY zeolite catalysts were investigated. Among these catalysts, HY zeolite with Si/Al molar ratio of 500 in Ni-Co over Al_2O_3-HY zeolite catalyst was selected to study effect of support ratio of Al_2O_3 and selected HY zeolite compared with bimetallic catalysts on either Al_2O_3 or HY zeolite support. Support ratio of Al_2O_3 and selected HY zeolite are as follows: 3:1, 1:1, 1:3. The results can be concluded as follows:

1. The bimetallic Ni-Co over Al_2O_3-HY zeolite catalyst with Si/Al molar ratio in HY zeolite of 500 exhibited higher both CH_4 and CO_2 conversions than the other catalysts with lower Si/Al molar ratio in HY zeolite. It showed the better catalytic performance because of higher metal dispersion on surface catalyst meaning high metal active sites and lower acidity on catalyst resulting greater affinity for CO_2 adsorption.
2. In comparison with support ratio of Al_2O_3 and HY500, Ni-Co over Al_2O_3-HY zeolite catalyst in support ratio of 1:3 achieved the highest both CH_4 and CO_2 conversions than the others because of the highest metal dispersion, lower acidity on catalyst, resulting greater affinity for CO_2 adsorption, and a shift of reduction temperature to lower temperature which are easy reducible to active metal.

3. In comparing catalysts with pure supports and mixed Al_2O_3-HY500 supports, the mixed supports possess higher amount of active sites and metal dispersion than pure supports, resulting higher both reactant conversion and product selectivity. Thus, the mixed supports had synergy between Al_2O_3 and HY500 which promoted each other leading to higher catalytic performance.

5.2 Recommendations

The future works are recommended to improve catalytic performance as follows:

1. Study stability in long term of catalysts for carbon dioxide reforming with methane.
2. Study the catalytic performance in different temperature reaction that is a one of the major factors of influence the activity of reaction.
3. Determine the amount of Ni and Co by XRF spectrometry.
4. Study the carbon deposition of spent catalysts by temperature-programmed oxidation techniques (TPO).

REFERENCES

[1] Usman, M., Wan Daud, W.M.A., and Abbas, H.F. Dry reforming of methane: Influence of process parameters—A review. Renewable and Sustainable Energy Reviews 45 (2015): 710-744.

[2] Gao, J., Hou, Z., Lou, H., and Zheng, X. Dry (CO2) Reforming. Fuel Cells (2011): 191-221.

[3] Alipour, Z., Rezaei, M., and Meshkani, F. Effect of alkaline earth promoters (MgO, CaO, and BaO) on the activity and coke formation of Ni catalysts supported on nanocrystalline Al2O3 in dry reforming of methane. Journal of Industrial and Engineering Chemistry 20(5) (2014): 2858-2863.

[4] Gangadharan, P., Kanchi, K.C., and Lou, H.H. Evaluation of the economic and environmental impact of combining dry reforming with steam reforming of methane. Chemical Engineering Research and Design 90(11) (2012): 1956-1968.

[5] Cai, W.-J., Qian, L.-P., Yue, B., and He, H.-Y. Rh doping effect on coking resistance of Ni/SBA-15 catalysts in dry reforming of methane. Chinese Chemical Letters 25(11) (2014): 1411-1415.

[6] Jabbour, K., El Hassan, N., Casale, S., Estephane, J., and El Zakhem, H. Promotional effect of Ru on the activity and stability of Co/SBA-15 catalysts in dry reforming of methane. International Journal of Hydrogen Energy 39(15) (2014): 7780-7787.

[7] Baktash, E., Littlewood, P., Schomäcker, R., Thomas, A., and Stair, P.C. Alumina coated nickel nanoparticles as a highly active catalyst for dry reforming of methane. Applied Catalysis B: Environmental 179 (2015): 122-127.

[8] Luisetto, I., Tuti, S., and Di Bartolomeo, E. Co and Ni supported on CeO2 as selective bimetallic catalyst for dry reforming of methane. International Journal of Hydrogen Energy 37(21) (2012): 15992-15999.

[9] San-José-Alonso, D., Juan-Juan, J., Illán-Gómez, M.J., and Román-Martínez, M.C. Ni, Co and bimetallic Ni–Co catalysts for the dry reforming of methane. Applied Catalysis A: General 371(1-2) (2009): 54-59.

[10] Therdthianwong, S. Synthesis gas production from dry reforming of methane over Ni/Al2O3 stabilized by ZrO2. International Journal of Hydrogen Energy 33(3) (2008): 991-999.

[11] Elsayed, N.H., Roberts, N.R.M., Joseph, B., and Kuhn, J.N. Low temperature dry reforming of methane over Pt–Ni–Mg/ceria–zirconia catalysts. Applied Catalysis B: Environmental 179 (2015): 213-219.

[12] Estephane, J., Ayoub, M., Safieh, K., Kaydouh, M.-N., Casale, S., and Zakhem, H.E. CO2 reforming of CH4 over highly active and stable yRhNix/NaY catalysts. Comptes Rendus Chimie 18(3) (2015): 277-282.

[13] Alotaibi, R., Alenazey, F., Alotaibi, F., Wei, N., Al-Fatesh, A., and Fakeeha, A. Ni catalysts with different promoters supported on zeolite for dry reforming of methane. Applied Petrochemical Research 5(4) (2015): 329-337.

[14] Inaba, M., Murata, K., Saito, M., Takahara, I., and Mimura, N. HYDROGEN PRODUCTION BY CONVERSION OF METHANE OVER NICKEL-SUPPORTED USY-TYPE ZEOLITE CATALYSTS. Reaction Kinetics and Catalysis Letters 77 (2002): 109-115.

[15] Dincer, I. and Joshi, A.S. Solar Based Hydrogen Production Systems. 1 ed. SpringerBriefs in Energy. Springer-Verlag New York, 2013.

[16] Chawl, S.K., George, M., Patel, F., and Patel, S. Production of Synthesis Gas by Carbon Dioxide Reforming of Methane over Nickel based and Perovskite Catalysts. Procedia Engineering 51 (2013): 461-466.

[17] Matsumura, Y. and Nakamori, T. Steam reforming of methane over nickel catalysts at low reaction temperature. Applied Catalysis A: General 258(1) (2004): 107-114.

[18] Gouveia Gil, A., Wu, Z., Chadwick, D., and Li, K. Ni/SBA-15 Catalysts for combined steam methane reforming and water gas shift—Prepared for use in catalytic membrane reactors. Applied Catalysis A: General 506 (2015): 188-196.

[19] Lyubovsky, M., Roychoudhury, S., and LaPierre, R. Catalytic partial "oxidation of methane to syngas" at elevated pressures. Catalysis Letters 99(3-4) (2005): 113-117.

[20] Lavoie, J.M. Review on dry reforming of methane, a potentially more environmentally-friendly approach to the increasing natural gas exploitation. Front Chem 2 (2014): 81.

[21] Al-Fatesh, A.S.A., Fakeeha, A.H., and Abasaeed, A.E. Effects of Selected Promoters on Ni/Y-Al2 O3 Catalyst Performance in Methane Dry Reforming. Chinese Journal of Catalysis 32(9-10) (2011): 1604-1609.

[22] Fakeeha, A.H., Khan, W.U., Al-Fatesh, A.S., and Abasaeed, A.E. Stabilities of zeolite-supported Ni catalysts for dry reforming of methane. Chinese Journal of Catalysis 34(4) (2013): 764-768.

[23] Wang, S., Lu, G.Q.M., and Millar, G.J. Carbon Dioxide Reforming of Methane To Produce Synthesis Gas over Metal-Supported Catalysts: State of the Art. Energy & Fuels 10 (1996): 896-904.

[24] Qilei Song, R.X., Li, Y., and Shen, L. Catalytic Carbon Dioxide Reforming of Methane to Synthesis Gas over Activated Carbon Catalyst. Industrial & Engineering Chemistry Research 47 (2008): 4349-4357.

[25] Trueba, M. and Trasatti, S.P. **γ**-Alumina as a Support for Catalysts: A Review of Fundamental Aspects. European Journal of Inorganic Chemistry 2005(17) (2005): 3393-3403.

[26] Joo, O.-S. and Jung, K.-D. CH4 Dry Reforming on Alumina-Supported Nickel Catalyst. Bulletin of the Korean Chemical Society 23 (2002): 1149-1153.

[27] Tao, Y., Kanoh, H., Abrams, L., and Kaneko, K. Mesopore-Modified Zeolites: Preparation, Characterization, and Applications. Chemical Reviews 106 (2006): 896-910.

[28] Lutz, W. Zeolite Y: Synthesis, Modification, and Properties—A Case Revisited. Advances in Materials Science and Engineering 2014 (2014): 1-20.

[29] KADUK, J.A. and FABER, J. CRYSTAL STRUCTURE OF ZEOLITE Y AS A FUNCTION OF ION EXCHANGE. THE RIGAKU JOURNAL 12 (1995): 14-34.

[30] Kulprathipanja, S. Zeolites in Industrial Separation and Catalysis. Wiley, 2010.

[31] Nickel Available from: https://en.wikipedia.org/wiki/Nickel

[32] Cobalt Available from: https://en.wikipedia.org/wiki/Cobalt

[33] Luengnaruemitchai, A. and Kaengsilalai, A. Activity of different zeolite-supported Ni catalysts for methane reforming with carbon dioxide. Chemical Engineering Journal 144(1) (2008): 96-102.

[34] Khajeh Talkhoncheh, S. and Haghighi, M. Syngas production via dry reforming of methane over Ni-based nanocatalyst over various supports of clinoptilolite, ceria and alumina. Journal of Natural Gas Science and Engineering 23 (2015): 16-25.

[35] Sarkar, B., et al. Reforming of methane with CO2 over Ni nanoparticle supported on mesoporous ZSM-5. Catalysis Today 198(1) (2012): 209-214.

[36] INOUE, H., HATANAKA, N., KIDENA, K., MURATA, S., and NOMURA, M. Reforming of Methane with Carbon Dioxide over Nickel-loaded Zeolite Catalysts. Journal of the Japan Petroleum Institute 45 (2002): 314-320.

[37] Sharifi, M., Haghighi, M., and Abdollahifar, M. Sono-dispersion of bimetallic Ni–Co over zeolite Y used in conversion of greenhouse gases CH4/CO2 to high valued syngas. Journal of Natural Gas Science and Engineering 23 (2015): 547-558.

[38] Sengupta, S., Ray, K., and Deo, G. Effects of modifying Ni/Al2O3 catalyst with cobalt on the reforming of CH4 with CO2 and cracking of CH4 reactions. International Journal of Hydrogen Energy 39(22) (2014): 11462-11472.

[39] Son, I.H., et al. Study on coke formation over Ni/γ-Al2O3, Co-Ni/γ-Al2O3, and Mg-Co-Ni/γ-Al2O3 catalysts for carbon dioxide reforming of methane. Fuel 136 (2014): 194-200.

[40] Estephane, J., et al. CO2 reforming of methane over Ni–Co/ZSM5 catalysts. Aging and carbon deposition study. International Journal of Hydrogen Energy 40(30) (2015): 9201-9208.

[41] Echeandia, S., et al. Enhancement of phenol hydrodeoxygenation over Pd catalysts supported on mixed HY zeolite and Al2O3. An approach to O-removal from bio-oils. Fuel 117 (2014): 1061-1073.

[42] Xu, B., Bordiga, S., Prins, R., and van Bokhoven, J.A. Effect of framework Si/Al ratio and extra-framework aluminum on the catalytic activity of Y zeolite. Applied Catalysis A: General 333(2) (2007): 245-253.

[43] Ay, H. and Üner, D. Dry reforming of methane over CeO2 supported Ni, Co and Ni–Co catalysts. Applied Catalysis B: Environmental 179 (2015): 128-138.

[44] Garrido Pedrosa, A.M., Souza, M.J.B., Melo, D.M.A., and Araujo, A.S. Cobalt and nickel supported on HY zeolite: Synthesis, characterization and catalytic properties. Materials Research Bulletin 41(6) (2006): 1105-1111.

[45] Alipour, Z., Rezaei, M., and Meshkani, F. Effect of Ni loadings on the activity and coke formation of MgO-modified Ni/Al2O3 nanocatalyst in dry reforming of methane. Journal of Energy Chemistry 23(5) (2014): 633-638.

[46] Rahmani, S., Rezaei, M., and Meshkani, F. Preparation of highly active nickel catalysts supported on mesoporous nanocrystalline γ-Al2O3 for CO2 methanation. Journal of Industrial and Engineering Chemistry 20(4) (2014): 1346-1352.

[47] Storck, S., Bretinger, H., and Maier, W.F. Characterization of micro- and mesoporous solids byphysisorption methods and pore-size analysis. Applied Catalysis A: General 137 (1998): 137-146.

[48] Foo, S.Y., Cheng, C.K., Nguyen, T.-H., and Adesina, A.A. Kinetic study of methane CO2 reforming on Co–Ni/Al2O3 and Ce–Co–Ni/Al2O3 catalysts. Catalysis Today 164(1) (2011): 221-226.

[49] Aw, M.S., Osojnik Črnivec, I.G., and Pintar, A. Tunable ceria–zirconia support for nickel–cobalt catalyst in the enhancement of methane dry reforming with carbon dioxide. Catalysis Communications 52 (2014): 10-15.

[50] Elordi, G., Olazar, M., Artetxe, M., Castaño, P., and Bilbao, J. Effect of the acidity of the HZSM-5 zeolite catalyst on the cracking of high density polyethylene in a conical spouted bed reactor. Applied Catalysis A: General 415-416 (2012): 89-95.

[51] Al-Dughaither, A.S. and de Lasa, H. HZSM-5 Zeolites with Different SiO2/Al2O3 Ratios. Characterization and NH3 Desorption Kinetics. Industrial & Engineering Chemistry Research 53(40) (2014): 15303-15316.

[52] Shirazi, L., Jamshidi, E., and Ghasemi, M.R. The effect of Si/Al ratio of ZSM-5 zeolite on its morphology, acidity and crystal size. Crystal Research and Technology 43(12) (2008): 1300-1306.

[53] Lovell, E., et al. CO2 reforming of methane over MCM-41-supported nickel catalysts: altering support acidity by one-pot synthesis at room temperature. Applied Catalysis A: General 473 (2014): 51-58.

[54] Zhang, J., Wang, H., and Dalai, A.K. Effects of metal content on activity and stability of Ni-Co bimetallic catalysts for CO2 reforming of CH4. Applied Catalysis A: General 339(2) (2008): 121-129.

[55] Jeong, H., Kim, K.I., Kim, D., and Song, I.K. Effect of promoters in the methane reforming with carbon dioxide to synthesis gas over Ni/HY catalysts. Journal of Molecular Catalysis A: Chemical 246(1-2) (2006): 43-48.

[56] Moradi, G., Khezeli, F., and Hemmati, H. Syngas production with dry reforming of methane over Ni/ZSM-5 catalysts. Journal of Natural Gas Science and Engineering 33 (2016): 657-665.

[57] Selvarajah, K., Phuc, N.H.H., Abdullah, B., Alenazey, F., and Vo, D.-V.N. Syngas production from methane dry reforming over Ni/Al2O3 catalyst. Research on Chemical Intermediates 42(1) (2016): 269-288.

[58] Fakeeha, A.H., Naeem, M.A., Khan, W.U., and Al-Fatesh, A.S. Syngas production via CO2 reforming of methane using Co-Sr-Al catalyst. Journal of Industrial and Engineering Chemistry 20(2) (2014): 549-557.

[59] Halliche, D., Cherifi, O., and Auroux, A. Microcalorimetric studies and methane reforming by CO2 on Ni-based zeolite catalysts. Thermochimica Acta 434(1-2) (2005): 125-131.

[60] Halliche, D., Cherifi, O., Taarit, Y.B., and Auroux, A. Catalytic reforming of methane by carbon dioxide over nickel-exchanged zeolite catalysts. Kinetics and Catalysis 49(5) (2008): 667-675.

[61] Ramírez, S., Schacht, P., and Ancheyta, J. Effect of Support Acidity on n-heptane Reforming over PtBeta zeolite+γAlumina Catalysts. Journal of the Mexican Chemical Society 49(3) (2005): 371-278.

[62] Huang, T., Huang, W., Huang, J., and Ji, P. High Stability of Ni-Co/SBA-15 Catalysts for CH4 Reforming with CO2. Energy Sources, Part A: Recovery, Utilization, and Environmental Effects 37(5) (2015): 510-517.

[63] Abdollahifar, M., Haghighi, M., and Babaluo, A.A. Syngas production via dry reforming of methane over Ni/Al2 O3 – MgO nanocatalyst synthesized using ultrasound energy. Journal of Industrial and Engineering Chemistry 20(4) (2014): 1845-1851.

[64] Takanabe, K., Nagaoka, K., Nariai, K., and Aika, K. Titania-supported cobalt and nickel bimetallic catalysts for carbon dioxide reforming of methane. Journal of Catalysis 232(2) (2005): 268-275.

[65] Aboonasr Shiraz, M.H., Rezaei, M., and Meshkani, F. Microemulsion synthesis method for preparation of mesoporous nanocrystalline γ-Al2 O3 powders as catalyst carrier for nickel catalyst in dry reforming reaction. International Journal of Hydrogen Energy 41(15) (2016): 6353-6361.

[66] Zhang, Z.L., Tsipouriari, V.A., Efstathiou, A.M., and Verykios, X.E. Reforming of Methane with Carbon Dioxide to Synthesis Gas over Supported Rhodium Catalysts- I. Effects of Support and Metal Crystallite Size on Reaction Activity and Deactivation Characteristics. Journal of Catalysis 158 (1996): 51-63.

[67] Edwin L. Kugler, D.B.D., Lawrence Norcio and Mahesh Iyer. Methane Reforming with Carbon Dioxide. Chemical Engineering, West Virginia University.

[68] Thongratkeaw, S. COMPARISON OF MONO METALLIC AND BIMETALLICS Co, Ni CATALYSTS SUPPORTED ON Al_2O_3/ZSM-5 FOR CO_2 REFORMING OF METHANE. Chemical Engineering Chulalongkorn University, 2015.

APPENDIX

APPENDIX A
CALCULATION FOR CATALYST PREPARATION

A.1 Preparation of the mixed Al_2O_3 and HY zeolite by sol-gel method

The preparation of Al_2O_3-HY zeolite supports with different Si/Al molar ratio of HY zeolite by sol-gel method are shown as follow:

Example The calculation for the preparation of Al_2O_3-HY500 support by sol-gel method are shown as follow:

Reagent:		
	HY zeolite	Si/Al molar ratio = 500
	Aluminum isoproproxide (>98%)	Molecular weight = 204.24 g/mol
	Ethanol (99%)	Molecular weight =
	Deionized water	Molecular weight = 18 g/mol
	Hydrochloric acid (37.7%)	Molecular weight =

Calculation:

For weight ratio of Al_2O_3:HY500 = 3:1

Based on 15 g of Aluminum isopropoxide

HY500 = $15\ g \times \frac{1}{3}$

= 5 g

For molar ratio of Al_2O_3:H_2O = 15:0.1

Aluminum isopropoxide = 0.1 mol

= 0.1 mol x 204.24 g/mol

= 20.424 g

H_2O = 15 mol

= 15 mol x 18 g/mol

= 270 g

Required aluminum isopropoxide = 15 g

So required H_2O = $\frac{15\ g \times 270\ g}{20.424\ g}$

= 198.3 g

For volume ratio of H_2O:Ethanol = 1:1

Density of H_2O = 1 g/cm^3

H_2O = 198.3 g x $\frac{1\ cm^3}{g}$

= 198.3 cm^3

So required ethanol = 198.3 cm^3 x $\frac{1}{1}$

= 198.3 cm^3

In case of Al_2O_3-HY15 and Al_2O_3-HY200, the method of preparing uses the same calculation which can use HY15 or HY200 instead of HY500.

A.2 Preparation of the bimetallic Ni-Co over Al_2O_3, HY zeolite, and mixed Al_2O_3 and HY zeolite by the incipient wetness impregnation method

Example The preparation of 5 wt.% Ni-5 wt.% Co/Al_2O_3-HY zeolite catalysts by the incipient wetness impregnation method are shown as follow:

Reagent:

Nickel (II) nitrate hexahydrate (98%) Molecular weight = 290.79 g/mol

Cobalt (II) nitrate hexahydrate (98%) Molecular weight = 291.03 g/mol

Calculation:

Based on 1 g of catalyst, 5 wt.% Ni-5 wt.% Co/Al_2O_3-HY zeolite catalyst contains 10 wt.% metal.

So, Ni = 0.05 g

Co = 0.05 g

Al_2O_3-HY zeolite required = 1 - 0.05 g - 0.05 g

= 0.9 g

5 wt.% Ni-5 wt.% Co/Al_2O_3-HY zeolite were prepared using $Ni(NO_3)_2.6H_2O$ and $Co(NO_3)_2.6H_2O$ as metal precursors.

$$Ni(NO_3)_2.6H_2O \text{ required} = \frac{\text{Ni required} \times \text{MW of } Ni(NO_3)_2.6H_2O}{\text{MW of Ni} \times 0.98}$$

$$= \frac{0.05 \text{ g} \times 290.73 \text{ g/mol}}{58.693 \text{ g/mol} \times 0.98}$$

$$= 0.243 \text{ g}$$

$$Co(NO_3)_2.6H_2O \text{ required} = \frac{\text{Co required} \times \text{MW of } Co(NO_3)_2.6H_2O}{\text{MW of Co} \times 0.98}$$

$$= \frac{0.05 \text{ g} \times 291.03 \text{ g/mol}}{58.933 \text{ g/mol} \times 0.98}$$

$$= 0.252 \text{ g}$$

APPENDIX B
CALIBRATION CURVES

The calibration curves are used for calculation the mole of methane and carbon dioxide as reactant gas, and hydrogen and carbon monoxide as main product gas in methane reforming with carbon dioxide.

The composition of reactant and main product gas were analyzed by Thermal Conductivity Detector-type gas chromatograph Shimudzu, GC-8A using porapack-Q and molecular sieve 5A as column.

The calibration curves exhibit area and mole of gas in x-axis and y-axis, respectively. The curves of methane, carbon dioxide, hydrogen and carbon monoxide are illustrated in figure B1-B4.

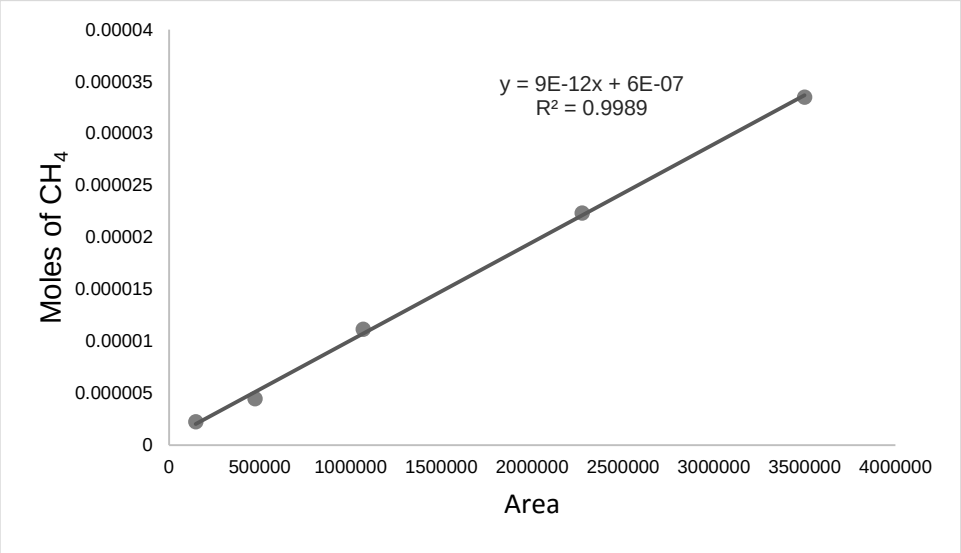

Figure B1 Calibration curve of methane.

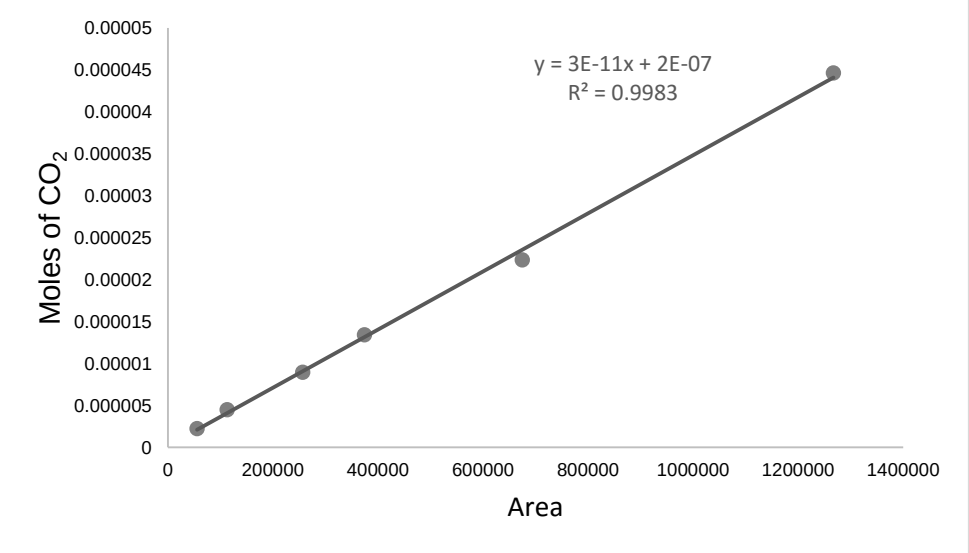

Figure B2 Calibration curve of carbon dioxide.

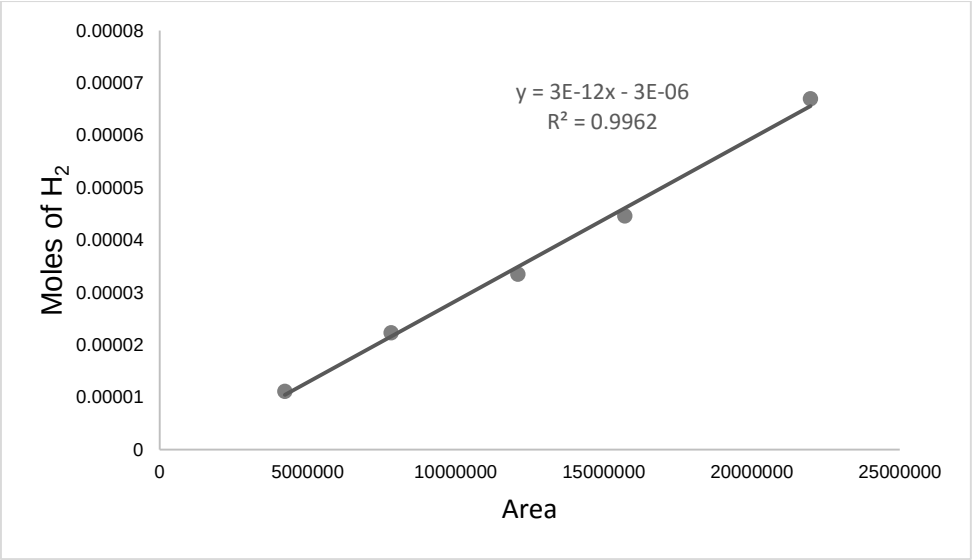

Figure B3 Calibration curve of hydrogen.

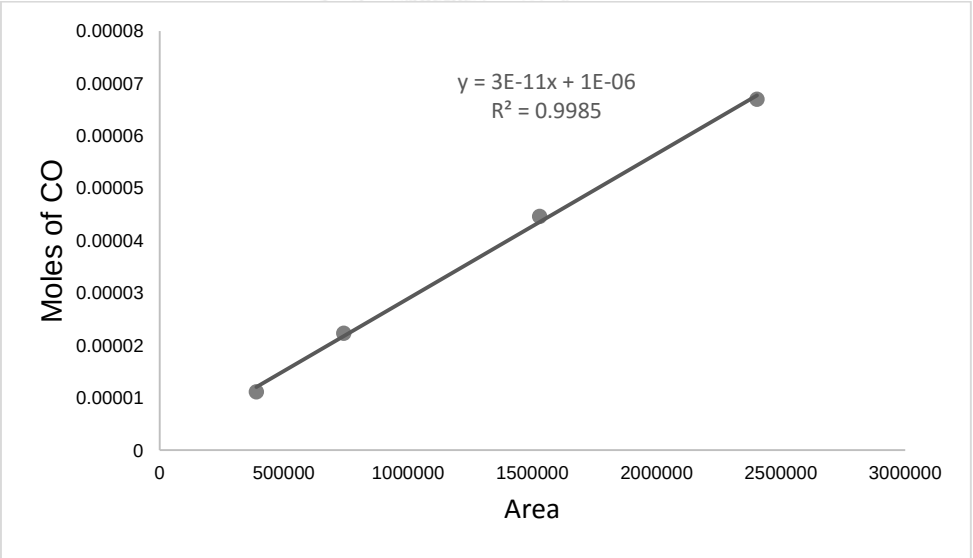

Figure B4 Calibration curve of carbon monoxide.

APPENDIX C

CALCULATION OF TOTAL ACID SITES OF CATALYST

Calculation of total acid sites of catalyst which were measured by Ammonia Temperature Programmed Desorption (NH_3-TPD) is shown as follows:

Example Ni-Co/1Al_2O_3-3HY500

Under area of the NH_3-TPD profiles of the sample = 3.26

Weight of sample = 0.1005 g

The mole of NH_3 was calculated from the calibration curve of NH_3 as formula:

The mole of NH_3 of the sample = 0.294 × 3.26

= 0.96 mmol NH_3

$$\text{The total acidity of sample} = \frac{\text{The mmol of } NH_3 \text{ of the sample}}{\text{Weight of sample}}$$

$$= \frac{0.96 \text{ mmol } NH_3}{0.1005 \text{ g}}$$

= 0.953 mmol NH_3/g

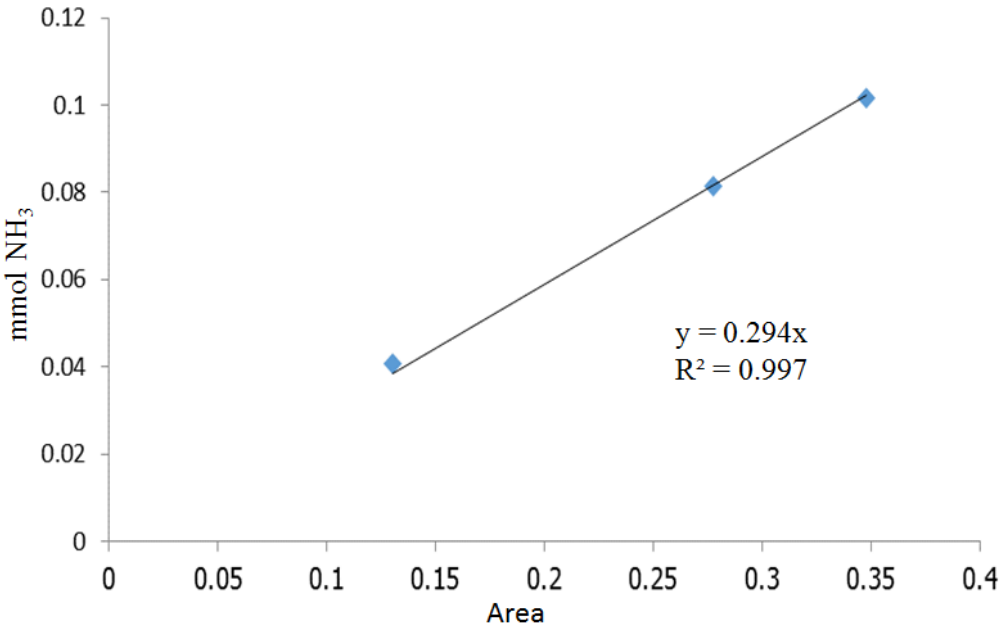

Figure C1 The calibration curve of ammonia from Micromeritics Chemisorp 2750.

APPENDIX D

CALCULATION OF ACTIVE SITE AND METAL DISPERSION OF CATALYST

Calculation of active site and metal dispersion of catalyst which were measured by Carbon monoxide chemisorption is shown as follows:

Example Ni-Co/1Al_2O_3-3HY500

Let	m	=	Weight of sample	=	0.05	g
	V_{inj}	=	Volume of injected CO	=	0.02	cm^3/g
	V_{ads}	=	Volume chemisorbed	=	0.772	cm^3/mol
	S_f	=	Stoichiometry factor	=	1	
	V_g	=	Molar volume of gas at STP	=	22414	cm^3
	MW	=	Molecular weight of metal	=	59	g/mol
	%M	=	% metal loading	=	10	%
	N_A	=	Avogadro's number	=	6.03×10^{23}	molecules/mol

Metal dispersion (%D)

$$\%D = S_f \times \frac{V_{ads}}{V_g} \times \frac{MW}{\%M} \times 100\% \times 100\%$$

$$= 1 \times \frac{0.772\ cm^3/g}{22414\ cm^3/mol} \times \frac{59\ g/mol}{10\%} \times 100\% \times 100\%$$

$$= 2.02\%$$

$$\text{Metal active site} = S_f \times \frac{V_{ads}}{V_g} \times N_A$$

$$= 1 \times \frac{0.772\ cm^3/g}{22414\ cm^3/mol} \times 6.02 \times 10^{23}\ molecules/mol$$

$$= 20.72 \times 10^{-18}\ molecules / g$$

APPENDIX E

CALCULATION OF CONVERSION AND SELECTIVITY

The methane and carbon dioxide conversions were calculated as defined equations as follows:

Methane conversion

$$X_{CH_4}(\%) = \frac{\text{Mole of } CH_4 \text{ in - Mole of } CH_4 \text{ out}}{\text{Mol of } CH_4 \text{ in}} \times 100\%$$

Carbon dioxide conversion

$$X_{CO_2}(\%) = \frac{\text{Mole of } CO_2 \text{ in - Mole of } CO_2 \text{ out}}{\text{Mol of } CO_2 \text{ in}} \times 100\%$$

The product selectivity based on mole of hydrogen and mole of carbon monoxide were calculated as defined equations as follows:

Hydrogen selectivity

$$S_{H_2}(\%) = \frac{\text{Mole of } H_2 \text{ out}}{\text{Mole of } H_2 \text{ out} + \text{Mole of CO out}} \times 100\%$$

Carbon monoxide selectivity

$$S_{CO}(\%) = \frac{\text{Mole of CO out}}{\text{Mole of } H_2 \text{ out} + \text{Mole of CO out}} \times 100\%$$

VITA

Miss Tipanate Chaovanich was born on January 2rd, 1992 in Bangkok, Thailand. She finished high school from Horwang School in 2010, and graduated in bachelor's degree from Faculty of Engineering in Chemical Engineering, Kasetsart University, Thailand in April 2014. She continued to study in Master's degree of Chemical Engineering, faculty of Engineering, Chulalongkorn University, Thailand in August 2014.

List of publication:

Tipanate Chaovanich, and Suphot Phatanasri, "Carbon dioxide reforming of methane for syngas production over Ni-Co catalysts supported on Al2O3-HY zeolite", proceeding of the Pure and Applied Chemistry International Conference 2016 (PACCON), Bangkok, Thailand, Feb. 9-11, 2016.